Review of Saturn's icy moons following the Cassini mission

Michele K. Dougherty[1] and Linda J. Spilker[2]

[1]The Blackett Laboratory, Physics Department, Imperial College London, UK

[2]The Jet Propulsion Laboratory, Pasadena, California, USA

1. Introduction to the Saturn System

The Saturn system is the most complex in our solar system, containing a central gas giant planet with a surprising axisymmetric internal planetary magnetic field, numerous rings and many satellites (both large and small) as well as a magnetospheric cavity within which the planet, its rings and the majority of the satellites are embedded (see numerous references within various books Burns, 1977; Gehrels and Matthews, 1984; Brown et al., 2009, Dougherty et al., 2009, Baines et al., 2017, Tiscareno and Murray, 2017, Schenk et al., 2017). Here we will focus on the icy satellites of Saturn and the understanding we have gained from the highly successful NASA-ESA Cassini-Huygens mission (hereafter referred to as Cassini) which has been in orbit around the Saturn system since mid-2004 with end of mission occurring on 15th September 2017 as Cassini plunges into Saturn to protect the ocean world Enceladus.

Prior to the space age which began in the 1960's all of our knowledge of Saturn, its rings and satellites arose from ground-based astronomy. Until the use of long exposure photographic plates revolutionised the search for new bodies in the solar system (the first being discovered using this technique was Phoebe at Saturn by Pickering in 1898 (Pickering, 1899)) all of the satellites of Saturn were only discovered when the rings of the planet were edge on to the Earth and hence the brightness from the rings did not interfere with the visibility of the objects. The first known moon of Saturn, Titan, was discovered by Christiaan Huygens in 1655, followed by four moons discovered by Giovanni Cassini, Iapetus (1671), Rhea (1672), Dione (1684) and Tethys (1684), (Cassini, 1686). It was more than a century later before William Herschel discovered the next of Saturn's moons, Mimas and Enceladus in 1789 (Herschel, 1790), followed by Hyperion in 1848 (Bond, 1848; Lassell (1848a)). It was John Herschel (Lassell, 1848b) who suggested that the satellites be named after deities associated with the Greek god Saturn. The tenth satellite of Saturn was discovered in 1966 by A. Dollfus when the rings were observed edge on near equinox and this satellite was later named Janus. A few years later it became clear that the 1966 observations of Janus could only be explained if a second satellite was present with a very similar orbit, now known as Epimetheus (the eleventh moon), the only known example of co-orbitals within the solar system. In 1980, three additional moons (Dione, Tethys and Calypso) were discovered from the ground and later confirmed by the Voyager spacecraft flybys of Saturn in 1980 and 1981, followed by the discovery of three additional moons during the Voyager flybys themselves, Atlas, Prometheus and Pandora. The eighteenth moon to be discovered prior to the Cassini-Huygens spacecraft launch from Cape Canaveral in October 1997, was Pan which was discovered from archival Voyager images in 1990. Due to the improving high resolution imagining techniques used on ground-based telescopes as well as

by the arrival of the Cassini spacecraft in orbit at Saturn the number of discoveries of satellites continued apace. To date there are fifty three confirmed moons at Saturn and another nine provisional moons, each of which has its own unique story.

Information on planetary satellites provides critical clues into understanding the solar system and how it formed. However, prior to the space age our knowledge of the physical properties of the known Saturnian moons began with the dynamical determinations of mass and for their sizes, only the Galilean satellites of Jupiter and Saturn's largest moon Titan were big enough and/or near enough to the Earth to enable their disk to be measured. The various indirect ground based techniques were perfected over the years but they all had uncertainties linked to them and the measurements only improved with the Pioneer and Voyager spacecraft flybys and then the orbital tour of Cassini.

Prior to the Voyager 1 and 2 flybys in 1980 and 1981, only Titan, the largest and outermost of the regular group (with nearly circular orbits close to the ring plane) and with a well determined atmosphere, as well as Iapetus, with a large and varying nearly circular orbit of high inclination and a puzzling large amplitude of its light variation (Morrison et al., 1975), were recognized as being unique. For the rest of the known moons there seemed to be little to separate them other than their size and orbital distance from their parent planet, Saturn. All of this changed following the Voyager 1 flyby of Saturn on 12th November 1980, when it became clear that there were distinctive and geologically active bodies (references within Gehrels and Matthews, 1984).

Figure 1 shows the orbital position, with respect to Saturn and the rings, of the satellites we will focus on in this review. They include the six intermediate sized icy moons (Mimas, Enceladus, Tethys, Dione, Rhea and Iapetus) as well as Hyperion and Phoebe which are two of the three from the irregular group of satellites (Iapetus being the third). We will also reference seven of the tiny ring-region moons (Pan, Daphnis, Atlas, Prometheus, Pandora, Janus and Epimetheus). Titan, the largest moon in the solar system and the only one with a dense Earth-like atmosphere will not be described here, however see recent publications and books (Brown et al., 2009).

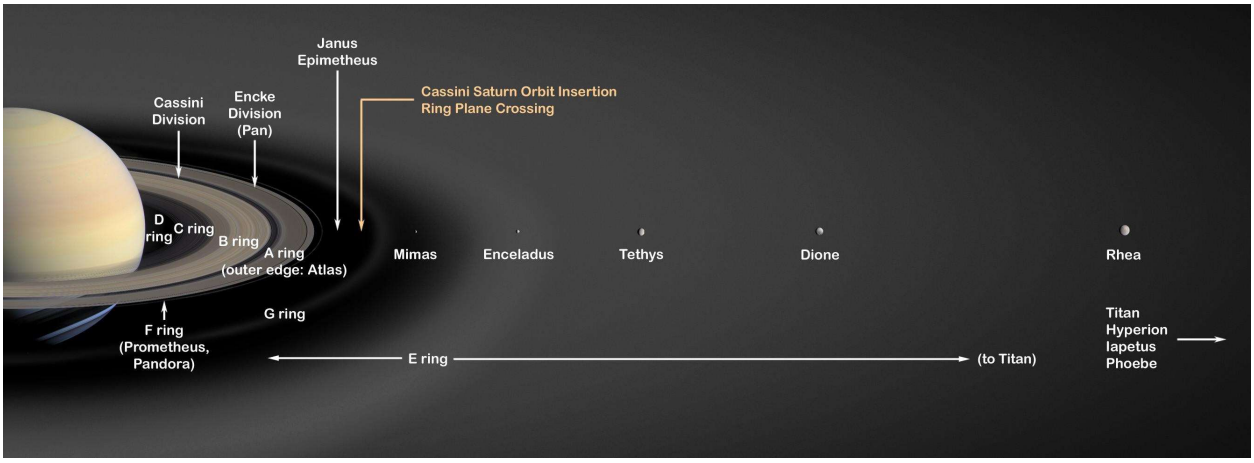


Figure 1: Schematic of Saturn, its rings and orbital position of the icy satellites which are the focus of this review. (PIA03550 (https://photojournal.jpl.nasa.gov/catalog/PIA03550), credited to NASA/JPL-Caltech).

2. Our knowledge prior to Cassini's arrival

Prior to the arrival of Cassini at the Saturn system on 1st July 2004 our knowledge of its moons had been derived from ground-based observations and brief spacecraft flybys of Saturn (those of Pioneer 11 in 1979 and Voyagers 1 and 2 in 1980 and 1981 respectively). Figure 2 reveals a Saturn family portrait of the planet and its principal moons created from images taken during the Voyager 1 November 1980 flyby. We will describe here our knowledge of the moons prior to Cassini Orbit Insertion beginning with the six intermediate-sized icy moons and in order of increasing radial distance from Saturn.

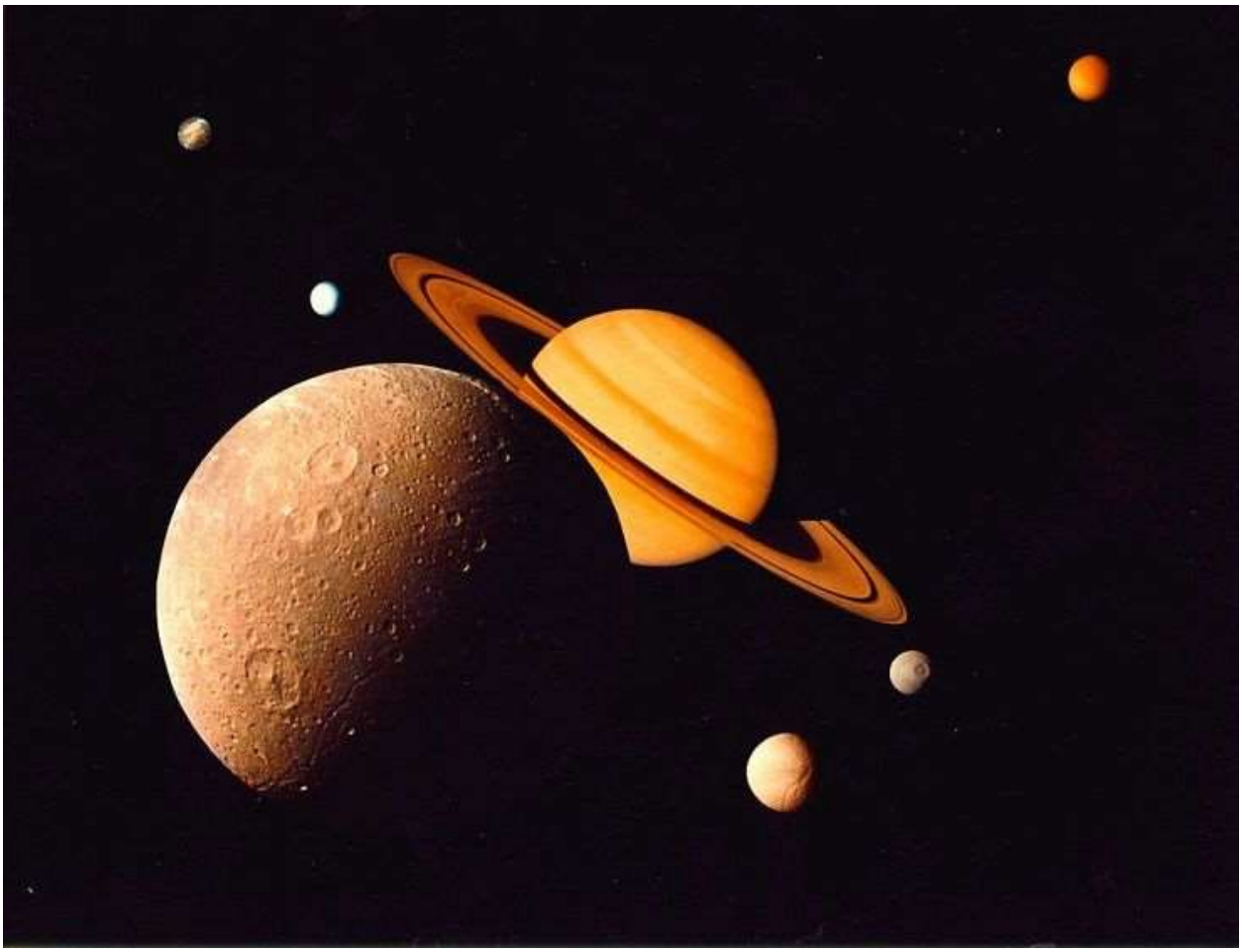


Figure 2: Saturn family portrait created from Voyager 1 images including the planet itself as well as Dione, Tethys, Mimas, Enceladus, Rhea and Titan (PIA01482

https://photojournal.jpl.nasa.gov/catalog/PIA01482), credited to NASA/JPL- Caltech).

2.1 Intermediate sized icy satellites

The six intermediate sized satellites are one of four classes of satellite at Saturn. The other three classes consist of large sized objects (Titan being the only one), captured objects (such as Phoebe) and the last being fragments of larger planetary bodies (see Burns, 1977). It was the Voyager spacecraft encounters in 1980 and 1981 which enabled geological studies of Saturn's satellites to begin. From photometry and spectral evidence the majority of the intermediate icy satellites have high surface albedos with water ice being the dominant spectrally active feature (except for Mimas and the dark hemisphere of Iapetus).

See Gehrels and Matthews (1984) for further details of the summaries provided in the sub-sections below.

2.1.1 Mimas

Mimas is the sm allest (diameter of 394km) and innermost of the classical regular or intermediate sized satellites. Its orbit lies between the tenuous G and E rings at a radial distance of 3.08Rs from Saturn (Herschel, 1790). Its surface is extremely heavily cratered and there is little indication of any major endogenic modifications and it has a fairly uniform albedo (or reflectivity). Its most striking feature is a well-preserved crater, named Herschel, 130km in extent and nearly centered on its leading hemisphere as well as covering a third of the surface. It is thought to be the result of an impact which nearly split the moon apart (Moore et al., 2004).

2.1.2 Enceladus

Enceladus is slightly larger than Mimas with a diameter of 502km and orbits Saturn at a radial distance of 3.95Rs. Both Enceladus and Mimas were discovered by W. Herschel in 1789 (Herschel, 1790). The remarkably high surface albedo of Enceladus has been known since ground-based observations of it were made (Slipher and Slipher (1914); Franz and Millis (1975) and this was confirmed by the Voyager flybys. It is deficient in large craters, a striking indication of large scale endogenic activity (especially when compared to Mimas close by) although there are some craters in its north polar region. The mid-latitudes and equatorial regions have vast crater-free smooth plains with a system of peculiar curvilinear ridges up to 1km in height (Smith et al., 1982). Photometric properties of its surface are remarkably uniform (Buratti, 1988) and it appears to have been extensively and recently resurfaced. Water ice was found to be the dominant spectrally active feature of the surface. It was postulated that the satellite may be the source of the E ring which has a peak in density near the orbit of Enceladus (Haff et al., 1983) and some of the questions raised following the Voyager flybys included whether the E ring is a recent phenomenon associated with the moon and whether there is an unexpectedly large internal heat source (Schenk, 2017).

2.1.3 Tethys

Tethys discovered by Cassini in 1684 (Cassini, 1686) orbits at 4.88Rs and is over twice the diameter of Enceladus (1060km). Like Dione and Rhea the moon exhibits terrains of different geological ages, for example north of the equator around a longitude of 60° the surface seems to be rough, hilly and densely cratered whereas a portion of the trailing hemisphere is clearly less rugged and lightly cratered (Stone and Miner, 1982; Moore et al., 2004). It seems to be much less active geologically than Enceladus, with heavily cratered terrain covering the majority of the surface and two outstanding topographic features, a large 500km diameter crater, known as Odysseus and a huge trough or rift zone (Ithaca Chasma) which extends over 270 degrees across the surface (Stone and Miner, 1981). The crater is the largest in our solar system and covers at least three quarters of the circumference of the moon.

2.1.4 Dione

Dione, also discovered by Cassini in the same year as Tethys (Cassini, 1686), orbits at a distance of 6.26Rs from Saturn and is slightly larger than Tethys (with a diameter of 1120km) but a higher bulk density (the highest well determined density amongst the inner satellites). Its surface has the highest brightness contrasts outside of Iapetus with the albedo being higher on the leading than trailing hemisphere with some evidence of wispy terrain (where the surface appears mottled with patches of different albedo, Morrison et al., 1984). Some of these wispy markings appear more like bright narrow

lines which extend into the leading hemisphere, some of which are associated with topographic features. Dione shows considerably more evidence of internal activity and a lower crater population than Rhea, the moon beyond it. There are extensive resurfaced plains and troughs or valleys hundreds of kilometers in length. The real surprise at Dione was the clear evidence for levels of endogenic activity exceeding in intensity and duration that observed on nearby and larger Rhea. The lack of correlation between observed geological history and expected thermal relaxation times represents one of the major geological challenges of the Voyager data for the regular satellites at Saturn (Morrison et al., 1984).

2.1.5 Rhea

Rhea is the largest of the intermediate sized satellites (close in size to Iapetus, both of which were discovered by Cassini in 1671 (Cassini, 1686)), with a diameter of 1530km and it orbits at a radial distance of 8.73Rs from Saturn. Images from Voyager revealed a bright heavily cratered surface (Moore et al., 2004) whose leading side is fairly uniform in brightness, with large craters (> 40km across) although in parts of the polar and equatorial regions the craters are smaller. These well-formed impact craters are similar to the highland provinces of the Moon and Mercury. The difference in size of the craters in the two areas may be an indication of a major resurfacing event at some stage in in Rhea's past (Morrison et al., 1984).

2.1.6 Iapetus

Iapetus, the last of the intermediate sized satellites, with a diameter of 1460km, has a large nearly circular high inclination (14.7°) varying orbit around Saturn (at a radial distance of 59Rs). Its orbital variation is due to the combined action from the Sun and Saturn's oblateness. It is best known for the puzzling large amplitude of its light variation (Morrison et al., 1975), with a leading hemisphere almost 25 times darker than its trailing hemisphere, similar in darkness to cometary nuclei and other primitive bodies. The dark material is reddish in color and carbon bearing (Morrison et al., 1984). There is virtually perfect longitudinal symmetry of dark material with respect to its direction of orbital motion which the Voyager data confirmed as well as the bright polar regions which were suggested from earlier photometric measurements. There is a large dark equatorial ring, some 300km in diameter, which interrupts the symmetry of the albedo boundary and the bright side of the surface is heavily cratered, especially the north polar region (Porco et al., 2005; Denk et al., 2010; Spencer et al., 2010). The density of Iapetus is very similar to the other icy satellites of Saturn and consistent with models where water ice is the primary constituent. As a consequence of the poor Voyager coverage of the leading hemisphere the nature and origin of the dark material remains uncertain. However, the strong symmetry with the direction of orbital motion points to some form of external control, such as dust from Phoebe or perhaps from an as yet undiscovered external satellite in a retrograde orbit?

2.2 Hyperion and Phoebe

These two moons have irregular orbits, Hyperion (discovered by W. Herschel in 1848, (Bond, 1848; Lassell (1848a)) is locked in a strong orbital commensurability with Titan which results in a variable orbital inclination and the outermost moon Phoebe (discovered by Pickering in 1898 (Pickering, 1899)) moves in a retrograde sense about Saturn in a large orbit of high inclination. Their orbital distances are 24.6Rs and 215 Rs respectively. Hyperion is irregularly shaped with many angular features and facets and is surely a fragmented remnant of a larger parent body. It has a dirty ice surface and a lower albedo and weaker ice bands than the inner regular satellites, with a rotation period that is apparently not synchronous (Matthews, 1992). Phoebe the most distant of Saturn's moons is nearly as dark as the dark

material on Iapetus and could potentially be its source. Its loose retrograde orbit and dark reddish color suggest it is a captured object with a primitive surface composition (Johnson et al., 2005). It is approximately spherical in shape with non-synchronous rotation. There are scattered brighter patches on darker areas however the resolution from the Voyager images could not reveal existence or not of craters.

2.3 Seven ring-region satellites

There are many satellites within Saturn's ring-region, in this article we will focus on seven of them, Pan which lies in the Encke division (discovered in 1990 using 10 year old Voyager data (Showalter, 1990)), Daphnis, which orbits in the Keeler gap in Saturn's outer A ring (discovered in 2005 by Cassini), Atlas an outer A ring shepherd (discovered in 1980 from Voyager 2 observations), Prometheus an inner F ring shepherd (also discovered in 1980 by Voyager 2 observations), Pandora an outer F ring shepherd (discovered in 1980 from Voyager 2 data), and Janus (Dollfus, 1966) and Epimetheus (Fountain and Larsen, 1977) which are co-orbitals. Hence observations from Voyager 2 led to the discovery of four new ring-region moons and sharpened our view of some that were previously known. The spacecraft also revealed how the gravitational pull of these satellites causes ripples in Saturn's rings and revealed that there were surprising gaps in the rings, some caused by moons embedded within them. One of these newly discovered moons only occurred some 10 years after the Voyager 2 flybys when in 1990 Showalter discovered Pan, the eighteenth and innermost moon of Saturn which orbits within and keeps open the Encke Gap in Saturn's rings via shepherding.

3. What we have learnt from Cassini

The Cassini-Huygens mission is a joint collaboration between NASA, ESA and the Italian Space Agency. Since July 2004 Cassini has returned a wealth of data about the Saturn system, yielding many new discoveries, including a new awareness of where and how life might exist beyond Earth. The results from the first four years of the mission invigorated icy satellite research as well as informing the mission trajectory for the extended missions which ensued. Over the course of its 13-year mission, Cassini has addressed a broad array of objectives across five interrelated science disciplines: Titan, Icy Satellites, Rings, Magnetosphere and Plasma Science, and Saturn. The Cassini orbiter flew with twelve science instruments: four optical remote sensing (ORS) instruments, two microwave remote sensing instruments, and six magnetosphere and plasma science (MAPS) instruments. Six instruments were on the ESA-built Huygens probe including visible and infrared spectrometers and imagers, and five in-situ instruments to measure the composition and characteristics of Titan's atmosphere and surface (Matson et al., 2002).

The Saturn year is almost 30 Earth-years long. Cassini's 13 years of observations within the Saturn system have spanned from winter in the northern hemisphere through equinox and mid-spring, and now northern summer in 2017. Completed in mid-2008, the Prime Mission began our exploration of the Saturn system, raising puzzling new questions such as the source of Enceladus' plume that focused the extended missions. The Equinox Mission continued observations throughout a two-year period surrounding the equinox crossing in August 2009. In 2010, the Cassini Solstice Mission began seven years of exploration characterized by equatorial orbits including many icy satellite targeted flybys; inclined orbits that provided optimal views of the rings and poles; and finally, highly inclined Ring-Grazing and Grand Finale orbits, diving between the innermost D ring and upper region of Saturn's atmosphere for the first time prior to the mission's end in 2017.

During its final year in orbit, Cassini witnessed the arrival of northern summer. Saturn's obliquity is almost 27°, and a unique combination of orbital geometry and near-solstice lighting conditions allowed studies of the complex seasonal changes that occurred throughout the Saturn system as the north polar regions of Saturn and its moons were warmed by sunlight for the first time during the mission. The final orbits are particularly well suited for studies of the rings, Titan's northern lakes, unexplored regions of the magnetosphere, the aurorae, Saturn's northern hexagon, and Saturn's atmosphere. The mission ends in September 2017, just after northern summer solstice.

The last year of the mission included Ring-Grazing orbits, a series of inclined orbits near the unusually dynamic F Ring, providing the best views of Saturn's inner moons, followed by the Grand Finale orbits, diving between the innermost D Ring and the upper portions of Saturn's atmosphere for the first time prior to the mission's end in 2017. These close orbits provide the highest resolution observations of both the rings and Saturn, and direct *in situ* sampling of the ring particles' composition, plasma, Saturn's exosphere and the innermost radiation belts. Saturn's gravitational field will be measured to unprecedented accuracy, providing information on Saturn's interior structure and mass distribution in the rings. Probing the magnetic field will give insight into the nature of the magnetic dynamo and the true rotation rate of Saturn's interior. The ion and neutral mass spectrometer will sniff the exosphere and upper atmosphere and examine water-based molecules originating from the rings. The cosmic dust analyzer will sample particle composition from different parts of the main rings.

The final 22 orbits bear some similarity to Juno's polar orbits at Jupiter; because they occur at the same time, scientists will have a rare opportunity to compare directly the internal structure of our two largest planets. Cassini will return its final bits of unique data on 15 September 2017 as it plunges into Saturn's atmosphere, vaporizing and satisfying planetary protection requirements. Cassini's many significant firsts include both icy satellite as well as other Saturn system discoveries.

3.1 Icy satellite discoveries

Discoveries/firsts made by Cassini linked to icy satellite science include geological activity at Enceladus, the origin of Iapetus' yin-yang surface solved and the first ever targeted flyby of the moon Phoebe. At Enceladus the unexpected discovery of an extensive water vapor and ice particle plume was such a surprise that future mission phases were reshaped to capitalize on this discovery. Cassini then proceeded to find a global ocean of liquid water with potential hydrothermal vents on the seafloor (see section 4.1 for a detailed discussion of our understanding of Enceladus following the Cassini orbital tour). Earth-based life depends on water, so the search for potential habitability has been extended to this small, bright moon.

The origin of Iapetus' two-faced, bright-dark surface has been unresolved since Iapetus was discovered almost 350 years ago, the Cassini spacecraft observations have now solved this puzzle. Dark, reddish dust that is eroded from the surface of the outer captured moon Phoebe and crosses Iapetus' orbital path is swept up and lands on the leading face of the moon. The dark areas absorb energy and become warmer, while the white areas remain cooler. Iapetus has both one of the brightest and darkest surfaces of any moon in our solar system.

As it entered the Saturn system in 2004, Cassini performed its first targeted flyby of one of the planet's moons, Phoebe, the largest of Saturn's outer or "irregular" moons. Phoebe is most likely a captured Kuiper Belt object, initially forming far beyond the orbit of Saturn and with a different origin from

Saturn's other inner, regular moons. It orbits Saturn in a retrograde direction. Phoebe is a very dark object, reflecting only about 4% of the sunlight that it receives. This was the only close flyby of one of the outer moons of Saturn.

Some of these early icy satellite discoveries resulting from Cassini observations drove the design of spacecraft orbits for the mission extensions that followed the Prime mission. The key icy satellite discovery that helped shape the extended missions were the unexpected findings about Enceladus. The prime mission had included just four close Enceladus flybys and numerous flybys of other moons as well. After the Enceladus discoveries in 2005, 19 more close flybys were added over the next nine years, including seven in the Equinox mission and 12 more during the Solstice mission.

Some of the most surprising scientific findings of the mission to date have resulted from encounters with Saturn's diverse and dynamic moons, in particular Enceladus. Each of Saturn's 62 moons is unique and there is a great deal of unexpected diversity among them, even among the outer captured moons. Many surprising discoveries including volcanic activity on Enceladus, the sponge-like appearance of Hyperion, and the equatorial ridge of Iapetus all of which will be discussed in the following sections. Studies of the icy satellites in the context of the Saturn system have enabled us to learn more about the history of the solar system.

4. Our understanding of the Saturn satellites to date

4.1 Enceladus

Enceladus, the brightest moon in our solar system, reflects almost 90% of the light it receives from the sun, and has puzzled scientists for decades. It is the sixth largest moon around Saturn, only about 500 km across, and is one of the five major inner moons, along with Mimas, Tethys, Dione and Rhea. Its orbit falls between Mimas and Tethys, and it is tidally locked like our own moon, always keeping the same side facing Saturn. It orbits Saturn once every 33 hours (Schenk et al., 2017). Enceladus is in a 2:1 orbital resonance with Dione, completing two orbits around Saturn for each orbit of Dione. This resonance excites Enceladus' orbital eccentricity, which results in tidal deformation of Enceladus. The heat dissipated from this deformation is the primary heat source that drives geological activity (Nimmo et al., 2014).

Parts of Enceladus' bright, icy surface are incredibly smooth and crater-free, indicating a youthful surface that was resurfaced in the geologically recent past. Other regions show craters up to 35 km in diameter. Other areas contain fissures and tectonic fractures, or smooth plains. Voyager images in the early 1980's gave us our first close look at this unusual world, embedded in the thickest part of Saturn's E ring. Since the Voyager flybys, scientists considered the possibility that Enceladus might be a geologically active world as well as the source of the E ring (Spahn et al, 2006, Kempf et al., 2010, Mitchell et al., 2015). Cassini's magnetometer data provided the first clues about the nature of this extraordinary world (Dougherty et al., 2006).

Cassini first flew by Enceladus in early 2005 (Spencer et al., 2009). During the first two flybys, the magnetometer (MAG) detected an unusual signature in the magnetic field near Enceladus (Dougherty et al., 2006). The team discovered that a barrier of some sort was bending the magnetic field around Enceladus, keeping the field away from the surface. That same barrier was also deflecting and slowing the magnetospheric plasma in a way that indicated water ions. Perhaps a tenuous atmosphere was

causing this effect, much like the gasses and icy particles from a comet also cause a magnetic field to stand off from its surface. These tantalizing results (Dougherty et al., 2006) had intrigued scientists so the MAG team convinced the project to fly even closer to Enceladus during its third flyby.

After the surprising science results from those early flybys, the focus of the Cassini mission was modified, and Cassini flew close to Enceladus a total of 23 times over the next decade to reveal the incredible nature of this active, dynamic world. With its powerful suite of complementary science instruments, Cassini soon revealed a giant plume of water ice and water vapor (Waite et al., 2006, 2009), salts and organic materials (Postberg et al., 2011) that spouts from a global, salty liquid water ocean (Thomas et al., 2015) beneath Enceladus' icy crust. Jets and curtains of gas and icy particles shoot from four long fractures near its south pole (Porco et al., 2006). These particles and gas provide a sample of the ocean beneath, which is mostly water but also contains a host of other molecules including organics, ammonia and salts (Waite et al., 2006, 2009). Some of these materials could only be formed as a result of hydrothermal activity (Waite et al., 2017), providing potential evidence for hydrothermal vents on Enceladus' seafloor. On Earth, life exists deep in the ocean around hydrothermal vents and the possibility exists that Enceladus' ocean may also be habitable. With its global liquid water ocean, unique chemistry and internal heat, Enceladus is a promising ocean world with nearly everything needed to support life, as we know it on Earth. The following sections describe some of Cassini's many findings about Enceladus.

4.1.1 Geologically Active Surface

Given its small size, large distance from the sun, and no atmosphere to insulate it, scientists thought Enceladus should have frozen solid long ago (Spencer et al., 2009). Instead, Cassini's flybys of Enceladus revealed a surprisingly active world. Geysers shoot from its south pole forming a huge plume of water vapor and icy particles (Porco et al., 2006). Some of these particles leave Enceladus and form the E ring (Mitchell et al., 2015). Enceladus is the smallest body found so far to have active cryovolcanism on its surface.

Early images of Enceladus revealed a bright, icy world much as photographed by Voyager. During the Voyager flybys Enceladus' south pole was in darkness while Cassini's early flybys showed a fully sunlit, and remarkable south polar region. Detailed Cassini images from the Imaging Sub-System (ISS) of Enceladus' south pole were first obtained in July 2005, (Porco et al., 2006), see Figure 3. These images showed a complex, youthful terrain that is almost entirely free of impact craters. This region is cut by large tectonic fractures and is the youngest surface on Enceladus. It includes a system of four nearly parallel fissures, nicknamed "tiger stripes", that may also be tectonic in origin and are centered near the pole (Helfenstein, 2010). The fissures are flanked on each side by 100-m tall ridges. Each "tiger stripe" is about 130 km long, 2-4 km wide, and each is separated by about 35 km. The fractures are about 300 meters deep, with V-shaped inner walls (Helfenstein, 2010).

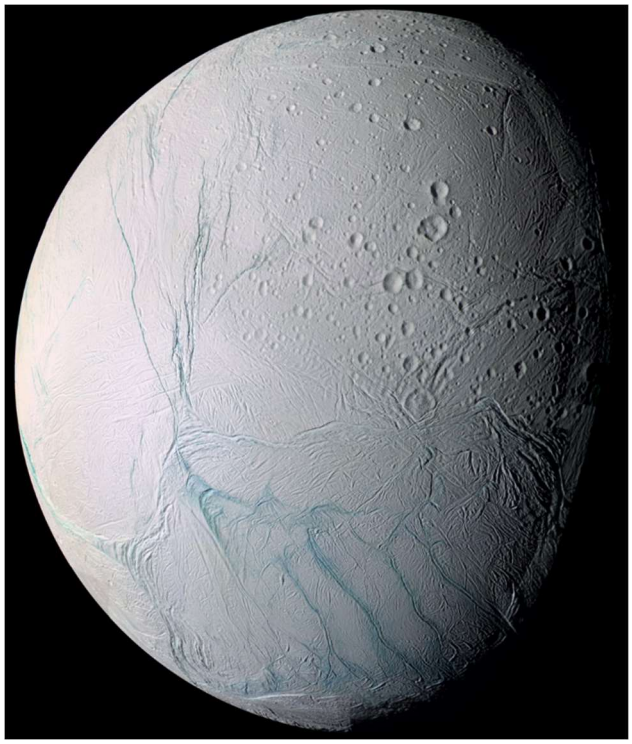


Figure 3: A high resolution view taken by the Imaging Sub-System on July 14, 2005. This large mosaic of 21 narrow-angle camera images have been arranged to provide a full-disk view of the anti-Saturn hemisphere on Enceladus. This mosaic is a false-color view that includes images taken at wavelengths from the ultraviolet to the infrared portion of the spectrum. In this false-color, many long fractures on Enceladus exhibit a pronounced difference in color (represented here in blue) from the surrounding terrain (Credit: NASA/JPL/Space Science Institute).

High-resolution images showed widespread deposits of fine-grained material along the ridges and terrain containing boulder-sized chunks of ice tens of meters in size (Martens et al., 2015). The tiger stripes are named after cities in the Arabian nights, Alexandria, Cairo, Bagdad and Damascus. Some high-resolution images also showed signs that the south polar icy crust has been spreading with time, much like some of the tectonic spreading we see on Earth (Yin and Pappalardo, 2015). On Enceladus, however, the spreading seems to be primarily in one direction.

The Cassini composite infrared spectrometer (CIRS) revealed another remarkable aspect of the south polar region, southward of 70° south latitude. The CIRS instrument created a thermal or heat map of the south polar region and found it was much warmer than anticipated if this region was heated solely from sunlight (Spencer et al., 2006), see Figure 4. CIRS measured Enceladus emission at mid- and far-infrared wavelengths to determine that the temperature in the "tiger stripe" region was hottest of all (Howett et al., 2011). The bulk of the heat is focused along the "tiger stripes" with temperatures of 115 – 190K, much warmer than the expected 65K for this area (Goguen et al., 2013, Spencer et al., 2013). The temperatures cool off quickly away from the main fissures. The heat source is coming from the interior of Enceladus, with the continuous release of over 16 gigawatts of energy, which is enough to power a city of about six million people.

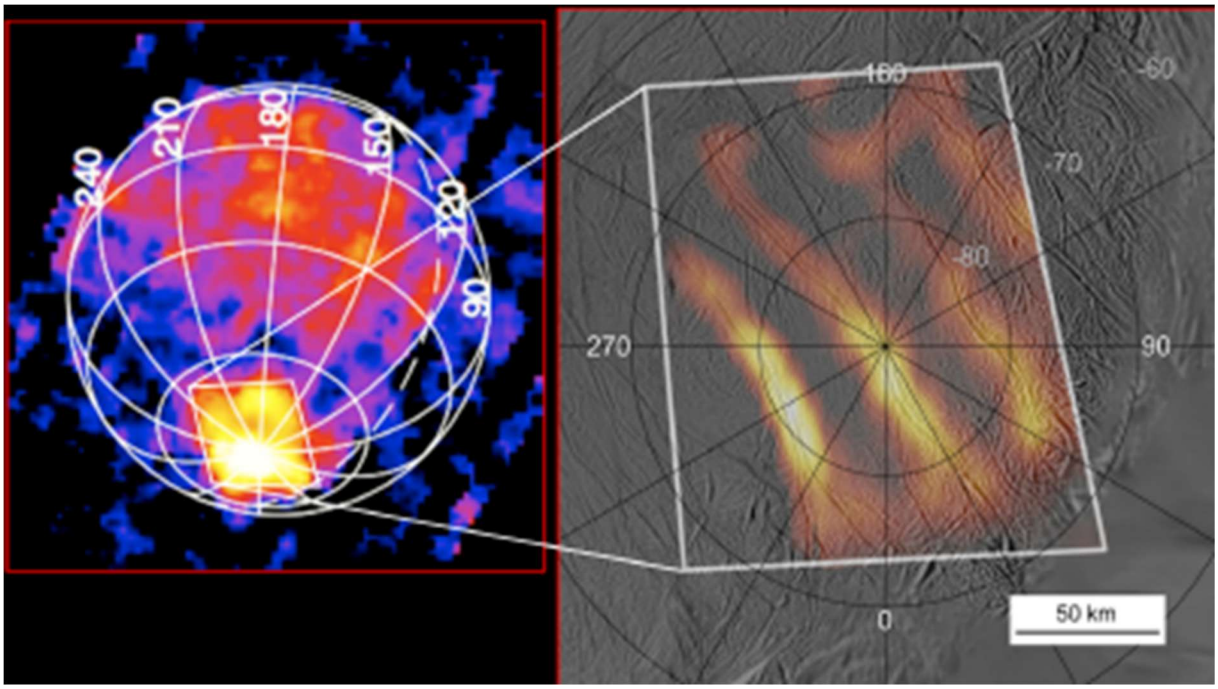


Figure 4: Left panel reveals a Mid-IR brightness temperature image of Enceladus 14th July 2005 flyby, showing the prominent south polar hot spot (PIA10361 Credit: NASA/JPL-Caltech)). Right panel reveals the brightness temperature contours derived from the observations superposed on an ISS base map, showing the spatial correlation of the hot material with the region containing the tiger stripe troughs (PIA09037 Credit: NASA/JPL/Space Science Institute).

Tidal heating and tidal stress provide sources for this heat (Tobie et al., 2008). Enceladus' orbit around Saturn is slightly elliptical as a result of its 2:1 orbital resonance with Dione. During its elliptical orbit Enceladus moves closer to, and then farther away from Saturn. Enceladus feels a stronger gravitational tug from Saturn when it is closer to the planet compared to when it is farther away. This oscillating gravitational tug or tidal forcing on Enceladus causes it to flex slightly, which produces tidal heating. These gravitational tides also produce stresses that crack the icy crust in places like the south pole. Tidal stress can pull these cracks open and closed during Enceladus' orbit around Saturn (Nimmo et al, 2014), generating friction, which could release some extra heat at the surface. Using current models, the total heat produced by tidal heating and stress can only explain a portion of the excess heat emanating from Enceladus' south pole. If the Dione-Enceladus interaction changes with time, more intense periods of tidal heating may be separated by more quiescent periods perhaps providing a mechanism to generate the necessary heat (Bland et al., 2012).

The north pole of Enceladus does not exhibit activity similar to its south pole. The north pole contains a large fracture that goes through the pole and exhibits numerous craters as well. Perhaps the crust is thicker in the north polar region which might prohibit similar activity. Other areas of Enceladus include smooth plains that typically have low relief and fewer craters than the cratered terrains (Kirchoff and Schenk, 2009) such as the north polar region. Some of these plains exhibit troughs and ridges as well as a lower crater density, indicating a younger surface than the cratered regions.

4.1.2 Active plume at south pole

A giant plume of water vapor gas and icy grains, fed by discrete jets and curtains of material emanating from each tiger stripe, extends thousands of kilometers into space (Porco et al., 2014, Spitale et al., 2015). The material shoots out of the tiger stripes at about 1.25 km/sec. A fair fraction of the material eventually re-impacts Enceladus after it escapes into Saturn orbit but some of the tiniest grains escape Enceladus' gravity and form Saturn's extended E ring (Spahn et al., 2006; Kempf et al., 2010; Mitchell et al., 2015). Cassini found that more than 90% of the material in the plume is water vapor. This gas lofts the particles into space where sunlight scatters off them and makes them visible to Cassini's cameras and spectrometers.

The Cassini imaging instrument, ISS, took the first images of Enceladus' plume in early 2005 (Porco et al., 2006) although concern about possible scattering inside the instrument at high phase angles delayed the announcement of plume detection until November 2005 when Cassini images clearly showed jets of icy particles spraying from Enceladus' south polar region (Spitale and Porco, 2007). These images showed the plume's detailed structure, revealing a number of individual jets within a larger plume that extended well above Enceladus' surface, see Figure 5.

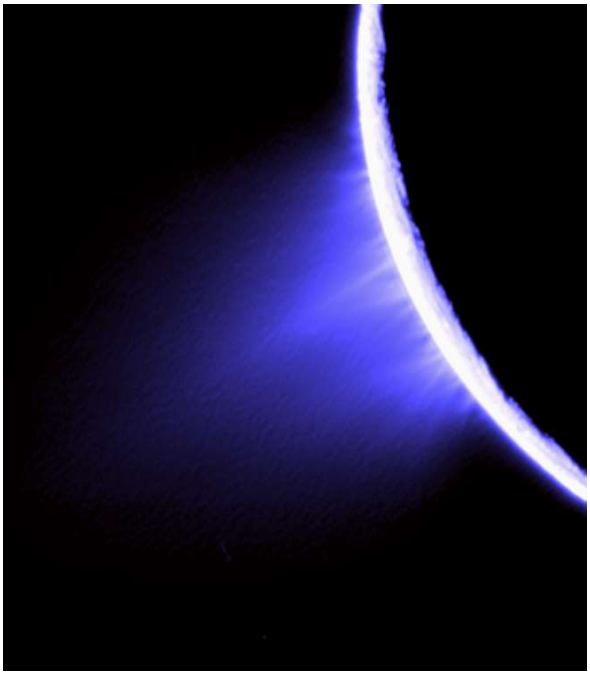


Figure 5: This false-color view was created by combining three clear filter images taken at nearly the same time to enhance the individual jets that compose the plume. The images were acquired with the Cassini spacecraft narrow-angle camera on Nov. 27, 2005 at a distance of approximately 148,000 kilometers from Enceladus (PIA08386 Credit: NASA/JPL/Space Science Institute).

Detailed analysis of Cassini images showed that the origin of some of the strongest jets is near the hottest spots CIRS measured along the tiger stripes. All of the jets appear to originate from locations along the four tiger stripes, and to date, one hundred individual jets have been mapped (Porco et al., 2014). Another source of Enceladus activity is curtain eruptions from material spouting along the length of the tiger stripe (Spitale et al, 2015). Some of the apparent jets may actually be phantom jets resulting from images taken along a fold or kink in the curtain that gives the optical illusion of a jet. Curtain

eruptions occur on Earth also when molten lava gushes out of a deep fracture and creates stunning curtains of fire such as those seen from some of the active Hawaiian volcanoes. The geysers on Enceladus are most likely a combination of jets and curtains. Output from these individual jets and curtains combine above Enceladus to form a single large plume.

The combined analysis of imaging, ultraviolet and mass spectrometer data suggests that the jets originate from pressurized chambers beneath the surface, similar to Earth's geysers. The intensity of the eruptions varies significantly as a function of the location of Enceladus in its orbit (Hedman et al, 2013; Nimmo et al., 2014). Visual and infrared mapping spectrometer (VIMS) data first showed that the particle plume is about three times brighter when Enceladus is at its most distant point in its orbit (apoapse) than at its closest point (periapse), consistent with the predicted opening of cracks near apoapse and closing of cracks near peripase (Hedman et al, 2013). Ultraviolet imaging spectrograph (UVIS) stellar occultation data, however, do not show this same large variation for the gas emission. UVIS saw only see about a 20% increase in the total amount of gas from apoapse to periapse of Enceladus' orbit. However, gas emission associated with a jet was four times higher for the same geometries. This four-fold increase in the jet's activity is what can loft more particles into space.

4.1.3 Subsurface global water ocean

The first indication that the Enceladus plume might be emanating from a liquid water source beneath its icy crust rather than from sublimation at its surface came from gravity measurements based on the change in the Doppler signal as Cassini flew close to Enceladus (Iess et al., 2014). The slight change in Doppler frequency indicates how strongly Cassini is affected by Enceladus' gravity. The initial gravity results pointed toward a liquid water source underneath the south pole.

Careful measurements on Enceladus images taken over the last decade showed a very slight libration, or wobble as Enceladus orbits Saturn (Thomas et al, 2015). The magnitude of that wobble can only be explained if Enceladus' outer icy shell is decoupled from its rocky core by a global ocean. The ocean is about 10 km deep underneath the south polar region, beneath an ice shell that is about 26 – 31 km thick. Enceladus' plume is being fed from this liquid water reservoir under the icy crust.

4.1.4 Plume composition and hydrothermal activity

Enceladus' plume is a mixture of gas and icy particles. Seven of Cassini's closest Enceladus flybys were targeted to fly through the plume to directly sample the plume material and determine its composition. Cassini's ion and neutral mass spectrometer (INMS) and UVIS measure gas and detected abundant water vapor. INMS discovered an unexpected mix of volatile gasses including small amounts of carbon dioxide, and simple hydrocarbons such as methane, propane, and acetylene (Waite et al., 2006, Waite et al., 2009). During Cassini's deepest dive through the plume in October 2015, the spacecraft flew through just 49 km above the surface where INMS discovered molecular hydrogen (H2) in the plume (Waite et al., 2017).

Cassini's cosmic dust analyzer (CDA) probes the icy particles and along with water found evidence for salt-rich ice grains containing sodium and potassium that are probably frozen droplets from a saltwater ocean underneath Enceladus' icy crust (Postberg et al., 2011). The salty minerals are created when liquid water is in contact with a mineral-rich rocky core and the salts are dissolved in the water. These grains also contain carbonates that provide a slightly alkaline pH value for the ocean (Postberg et al., 2009, Glein et al., 2015).

CDA also discovered tiny grains of silica, only 6 to 9 nanometers in size, even before Cassini entered Saturn's orbit in 2004 (Hsu et al., 2015). After careful study, the CDA team concluded that these tiny grains must originate inside Enceladus' ocean. The most common way to form silica grains this tiny on Earth is hydrothermal activity. Cold slightly alkaline and salty water is heated almost to the boiling point inside Enceladus' rocky core where it becomes super-saturated with silica and other minerals. This hot water undergoes a large temperature drop as it shoots out of hydrothermal vents and encounters the cold water. Tiny silica grains condense, ultimately being ejected into Enceladus' plume. Deep in Earth's oceans, hydrothermal vents called "white smokers" like "Lost City" also form tiny grains of silica in this way.

Other byproducts of hydrothermal activity, including methane and molecular hydrogen, have also been found in the Cassini data. Methane and molecular hydrogen are particularly abundant in Enceladus' plume. At the high pressures expected in Enceladus' oceans icy materials called clathrates can form and imprison molecules of methane or hydrogen within a crystalline structure of water ice. This clathrate process is so efficient at removing methane (Bouquet et al., 2015) and hydrogen (Waite et al., 2017) from the ocean that another explanation is needed to explain the abundance of methane and hydrogen observed by Cassini in the plume. Active hydrothermal processes could produce methane and hydrogen faster than it is being converted into clathrates and produce the excesses being observed. Molecular hydrogen provides a geochemical energy source by reacting with carbon dioxide to release a burst of energy that can be used by microbes, if any exist in Enceladus' ocean.

4.1.5 Plume creates E ring and coats surfaces of Saturnian moons

The plume material that escapes Enceladus's gravity leaves the moon and forms Saturn's E ring (Mitchell et al., 2015). The E ring consists of tiny micron and sub-micron particles of water ice, containing silicates, carbon dioxide and ammonia (Spahn et al., 2006; Kempf et al., 2010). The E ring is densest at Enceladus, and is spread throughout the Saturnian system, between the orbits of Mimas and Titan. Unlike Saturn's main rings, the E ring is more than 2000 kilometers thick and increases in thickness with its distance from Enceladus. Tendril-like structures have been observed within the E ring and can be traced back to jets emanating from the south pole (Mitchell et al., 2015). The tiny particles in the E ring are unstable, with a lifespan short enough that they must be continuously replenished for the E ring to continue to exist (Spahn et al., 2006).

E ring particles accumulate on the moons that orbit within it, including Mimas, Enceladus, Tethys, Dione and Rhea (Schenk et al., 2011). Bright E ring grains coat the surfaces of the tiny Trojan moons Telesto, Calypso, Helene and Polydeuces, and smooth out their surface features. E ring grains bombard the leading sides of Tethys and Dione, and the trailing side of Mimas (Hendrix et al., 2012). In the ultraviolet, the hemispheres bombarded by E ring grains are brighter than the opposite hemispheres, so Tethys and Dione have brighter leading hemispheres, and Mimas' trailing hemisphere is brighter. Enceladus itself displays variations in the thickness of its surface deposits (Hendrix et al., 2012). Global color mosaics show regions of enhanced deposits that are in agreement with CDA models of icy grain deposition (Schenk et al., 2011).

As Cassini first approached Saturn, UVIS found that the Saturn system was filled with oxygen atoms (Esposito et al., 2005). At that time, early in the mission, the source of oxygen was a puzzling. After discovering the plume, we now know that the Enceladus water vapor in Saturn's magnetosphere is

broken down into oxygen and hydrogen, providing both to the Saturn system (Waite et al., 2006, 2009). These materials react with other moons in the Saturn system, influencing their surfaces.

4.1.6 Enceladus interior: differentiated

Before the Cassini mission very little was known about the interior of Enceladus. A number of Enceladus flybys were dedicated to radio science and provided the effects of Enceladus' gravity on Cassini, yielding a mass for Enceladus (Iess et al., 2014). The mass and shape provided a density of 1.61 g/cm3, which is much higher than Saturn's other mid-sized icy satellites indicating that Enceladus contains larger amounts of silicates and iron. Gravity measurements also showed that the density of the core is low, indicating that the core contains water in addition to silicates and iron (Iess et al., 2014). High-resolution observations of the surface including images and spectra, indicated internal activity and thermal evolution (Howett et al., 2011, Spencer et al., 2013), providing additional evidence for a differentiated interior. Cassini observations have shown that Enceladus is a differentiated body with a liquid water ocean (McKinnon et al., 2015, Thomas et al., 2015). This combination provides the potential for ocean water to circulate within the rock. The heated water could pick up elements like silica, potassium, phosphorous, and sulfur, elements that are key for life as we know it.

4.1.7 Plasma ionization

Enceladus provides a unique laboratory for monitoring the unusual behavior of plasma, or hot ionized gas, in its vicinity. Enceladus is a major source of the ionized material that fills Saturn's magnetosphere (Coates et al., 2010, Hill et al., 2012). About 100 kilograms of water vapor per second spray out from the cracks at the south pole (Hansen et al, 2006, Hansen et al., 2011). The water vapor is converted into charged particles that interact with the plasma in Saturn's magnetosphere.

Cassini's fields and particles instruments have shown that the usual heavy and light charged particles in normal plasma are actually reversed near Enceladus' plume and that the dust grains are negatively charged (Morooka et al., 2011, Hill et al., 2012). The nature of this unique gas-dust-plasma mixture has been revealed over the course of Cassini's 13-year mission with data from multiple instruments, including the Cassini plasma spectrometer (CAPS), magnetometer (MAG), magnetospheric imaging instrument (MIMI), and the radio and plasma wave science instrument (RPWS).

4.1.8 Plume gas plume density

Using its ultraviolet imaging spectrograph (UVIS) Cassini was able to measure the amount of water vapor erupting from the geysers by monitoring a bright star as it passed behind the plume of gas and dust spewing from Enceladus (Hansen et al, 2006, Hansen et al., 2011). These measurements offered new insights on geologic activity happening beneath Enceladus' surface.

Other instruments on Cassini have observed that the number of water ice grains being ejected from the small moon was three times greater when Enceladus was farthest from Saturn in its orbit compared to when it was closest (Hedman et al., 2013, Nimmo et al., 2014). The UVIS instrument only measured a 20% increase with orbital position in the total amount of gas. However, when Cassini flew over one of Enceladus' active jets, UVIS measured that the jet was four times more active than the background water vapor. The active jets may be responsible for greater increase in particle emission as Enceladus orbits Saturn. Tidal forcing from Saturn may be responsible for slightly opening or closing the jets as Enceladus orbits the planet leading to increasing and decreasing particle flow.

4.1.9 Summary

Enceladus discoveries have changed the direction of planetary science. Multiple discoveries have increased our understanding of Enceladus, including the plume venting from its south pole; hydrocarbons in the plume; a global, salty ocean and hydrothermal vents on the seafloor. They all point to the possibility of a habitable ocean world well beyond Earth's habitable zone. Planetary scientists now have Enceladus to consider as a possible habitat for life. However, the Cassini spacecraft does not carry instruments to look for life so the search for life will require a future mission.

4.2 The other icy moons of Saturn

Following on from the initial discoveries made during the first 4 years of the Cassini orbital tour at Saturn, the focus in the extended missions were driven by the new knowledge we obtained. For the icy satellites the standout moon has been Enceladus as described in the section above but numerous other surprising discoveries at the other icy satellites have been made by Cassini (Jaumann et al., 2009). These include the sponge-like appearance of Hyperion (Thomas et al., 2007), and the equatorial ridge of Iapetus (Porco et al., 2005). The bright ray system on Rhea caused by a relatively recent impact, while the wispy streaks on Dione and Rhea which are tectonic in origin. The dark material on Iapetus, which seems to be only a thin surface coating, is composed of organics, with several of the spectral features of the material matching that seen on some of the other moons, such as Phoebe, Hyperion, Dione and Epimetheus as well as in the F ring and Cassini division, with the implication being that this material is found throughout the Saturn system. For Phoebe it has been confirmed that the dark material seems to have come from outside of the Saturn system (Cruikshank et al., 2008). The improved resolution and global mapping coverage of Cassini confirmed the abundance of impact craters on all satellites (Done et al., 2009) and has also revealed rather varied degrees of endogenic activity of Tethys, Rhea and Dione. All of the major satellites of Saturn (except for Hyperion) are synchronously locked, with the result that one hemisphere always faces Saturn. The importance of the icy satellites is that they allow us to gain a better understanding of the geological diversity of the different moons and how they interact within the complex Saturn system. A list of the targeted flybys (T) as well as the closest non-targeted (nT) Mimas flyby is shown in Table 1 detailing the date of the flyby, orbit number and flyby altitude. Table 2 reveals the known parameters of the satellites.

Target	Rev	Epoch (SCET)	Date (SCET)	Alt. (km)	T/nT
PHOEBE	0	2004-163T19:33	11 Jun 2004 19:33	2068	T
ENCELADUS	3	2005-048T03:30	17 Feb 2005 03:30	1261	T
ENCELADUS	4	2005-068T09:08	09 Mar 2005 09:08	497	T
ENCELADUS	11	2005-195T19:55	14 Jul 2005 19:55	166	T
HYPERION	15	2005-269T02:24	26 Sep 2005 02:24	479	T
DIONE	16	2005-284T17:52	11 Oct 2005 17:52	499	T
RHEA	18	2005-330T22:37	26 Nov 2005 22:37	504	T

IAPETUS	49	2007-253T14:15	10 Sep 2007 14:15	1622	T
ENCELADUS	61	2008-072T19:06	12 Mar 2008 19:06	48	T
ENCELADUS	80	2008-224T21:06	11 Aug 2008 21:06	49	T
ENCELADUS	88	2008-283T19:06	09 Oct 2008 19:06	25	T
ENCELADUS	91	2008-305T17:14	31 Oct 2008 17:14	169	T
ENCELADUS	120	2009-306T07:41	02 Nov 2009 07:41	99	T
MIMAS	126	2010-044T17:22	13 Feb 2010 17:22	9547	nT
ENCELADUS	121	2009-325T02:09	21 Nov 2009 02:09	1597	T
RHEA	127	2010-061T17:40	02 Mar 2010 17:40	102	T
DIONE	129	2010-097T05:16	07 Apr 2010 05:16	506	T
ENCELADUS	130	2010-118T00:10	28 Apr 2010 00:10	100	T
ENCELADUS	131	2010-138T06:04	18 May 2010 06:04	437	T
ENCELADUS	136	2010-225T22:30	13 Aug 2010 22:30	2555	T
ENCELADUS	141	2010-334T11:53	30 Nov 2010 11:53	46	T
ENCELADUS	142	2010-355T01:08	21 Dec 2010 01:08	48	T
RHEA	143	2011-011T04:53	11 Jan 2011 04:53	70	T
ENCELADUS	154	2011-274T13:52	01 Oct 2011 13:52	99	T
ENCELADUS	155	2011-292T09:22	19 Oct 2011 09:22	1231	T
ENCELADUS	156	2011-310T04:58	06 Nov 2011 04:58	497	T
DIONE	158	2011-346T09:39	12 Dec 2011 09:39	101	T
ENCELADUS	163	2012-087T18:30	27 Mar 2012 18:30	74	T
ENCELADUS	164	2012-105T14:01	14 Apr 2012 14:01	74	T
ENCELADUS	165	2012-123T09:31	02 May 2012 09:31	73	T
RHEA	183	2013-068T18:17	09 Mar 2013 18:17	997	T
DIONE	217	2015-167T20:11	16 Jun 2015 20:11	516	T
DIONE	220	2015-229T18:33	17 Aug 2015 18:33	479	T

ENCELADUS	223	2015-287T10:41	14 Oct 2015 10:41	1845	T
ENCELADUS	224	2015-301T15:22	28 Oct 2015 15:22	49	T
ENCELADUS	228	2015-353T17:49	19 Dec 2015 17:49	4999	T

Table 1: Details of all of the targeted satellite flybys from Cassini and the closest non-targeted Mimas flyby.

Name	**Orbit Semimajor Axis**	**Orbit Period**	**Mean Diameter**
	(km)	**(days)**	**(km)**
Pan	133,580	0.575	27
Daphnis	136,505	0.594	8
Atlas	137,670	0.602	30
Prometheus	139,380	0.613	85
Pandora	141,720	0.629	80
Epimetheus	151,410	0.694	117
Janus	151,460	0.695	178
Aegaeon	167,494	0.808	<1
Mimas	185,539	0.942	397
Methone	194,440	1.010	3
Anthe	197,655	1.037	2
Pallene	212,280	1.154	4
Enceladus	238,037	1.37	504
Tethys	294,672	1.888	1062
Telesto	294,710	1.888	24
Calypso	294,710	1.888	19
Polydeuces	377,200	2.737	3
Dione	377,415	2.737	1123
Helene	377,420	2.737	36
Rhea	527,068	4.518	1528

Titan	1,221,865	15.95	5151
Hyperion	1,500,934	21.28	272
Iapetus	3,560,851	79.33	1468
Phoebe	12,947,913	550.3	213

Table 2: Known parameters of the Saturnian satellites.

We will now deal with each of the satellites in turn, starting with Mimas the closest in icy satellite and moving outwards with distance away from Saturn.

4.2.1 Mimas

There have been four untargeted and therefore rather distant flybys of this icy moon whose main feature is that of the prominent crater Herschel (which has a diameter ~120km and a depth ~11km). In addition the surface is crossed by number of linear almost parallel troughs that are thought to potentially be the consequence of fractures on a global scale as a result of the Herschel impact event (McKinnon, 1985). However these features do not form a simple radial or concentric pattern which would be expected if they were related to an impact event and so they may simply be a random feature arising as a result of the freeze expansion of the interior (Jaumann et al., 2009) It will take closer, more targeted flybys of Mimas in the future for a better understanding of these features as well as the interior of the moon to be gained. The Cassini surface spectra of Mimas confirm that the surface is dominated by water ice.

Figure 6 reveals an ISS image of Mimas, as well as a temperature map of the surface from CIRS. Instead of the smoothly varying temperatures peaking in the early afternoon near the equatorial region as one might expect, the warmest region was found to arise in the morning, along one edge of the disk of the moon, in a Pac-Man shape (Howett et al., 2011). The peak temperature is of order 92 degrees Kelvin with the rest of the moon being much colder around 77 degrees Kelvin. There is a small warm dot (84 degrees Kelvin) close to the Herschel crater which can be explained as a result of heat being trapped by the tall crater walls. The hot sharp and V-shaped pattern of the thermal anomaly is more difficult to interpret however and is potentially revealing different textures on the surface. The boundary does not correspond to any clear change in surface albedo suggesting therefore that the thermal inertia variations are probably responsible for the anomaly (Spencer et al., 2010). Global color maps of Mimas (Schenk et al. 2011) reveal an unusual blue region that is similar in shape and size and may have the same cause, and it was noted that the shape is consistent with its formation being caused by irradiation of Mimas' surface by high-energy electrons. What the mechanism is that would enable such high thermal inertias to be produced by electron irradiation is as yet unknown.

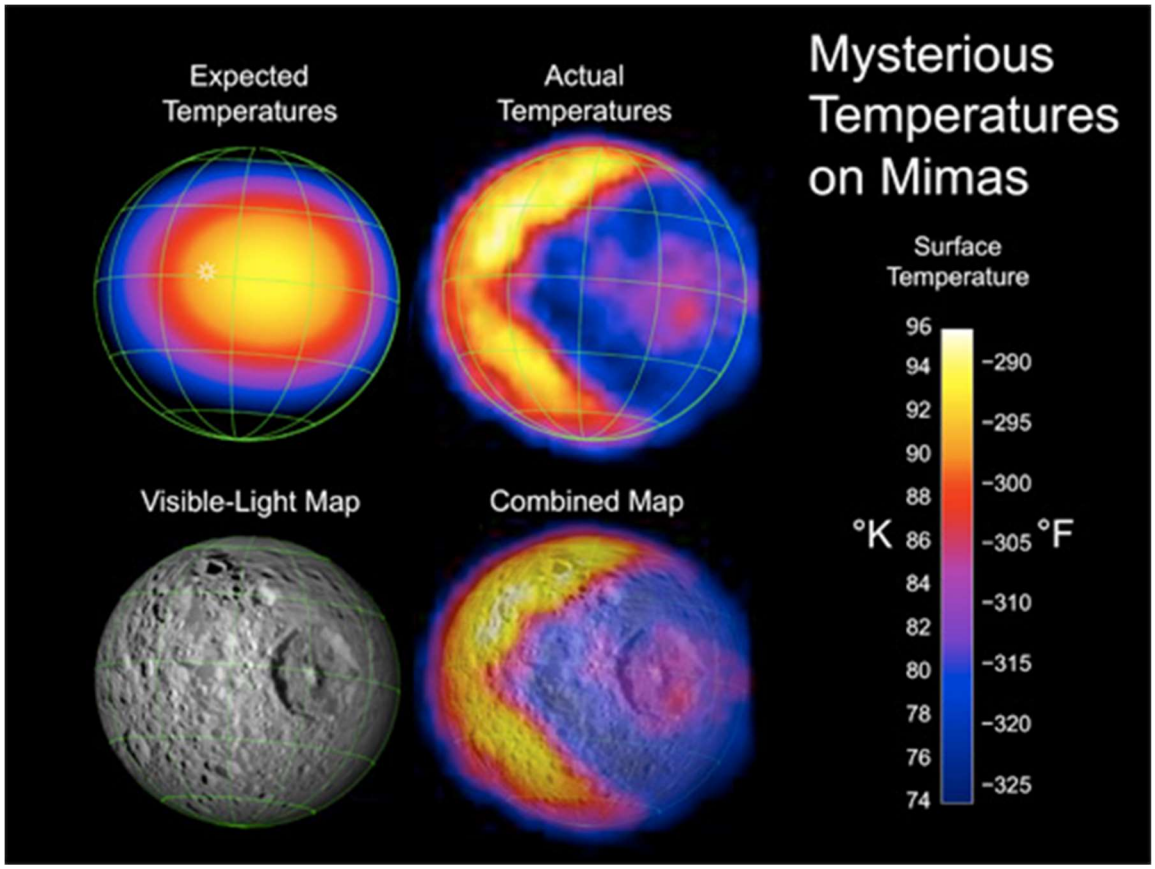


Figure 6: This montage reveals data obtained on 13th February 2010 from ISS and CIRS. The upper left image shows the expected distribution of temperatures. The white sun symbol shows the point where the sun is directly overhead, which is at midday close to the equator. The upper right image reveals the temperature actually measured. The lower two panels compare the temperature map to Mimas' appearance in ordinary visible light, with the map used to created by a mosaic of images taken by ISS on previous flybys of Mimas (PIA12867 Credit:Nasa/JPL-Caltech).

4.2.2 Tethys

At Tethys, there has been one targeted and seven non-targeted flybys. The surface of this moon is dominated by 2 large features, a large valley known as Ithaca Chasma (Smith et al., 1982) which spans three quarters of the globe of the moon and a giant impact basin known as Odysseus which is of order 400km in diameter. The size of such an impact would have shattered a solid body and so it is likely that Tethys was still partially molten when the impact took place. The large valley feature is 100 kilometers wide, 3 to 5 kilometers deep, and extends 2000 kilometers. There are a number of theories to explain its formation including that it may have been caused by expansion of internal liquid water as it froze into ice after the surface had already frozen or an alternate theory is that the impact that created the Odysseus Crater also generated forces that created Ithaca Chasma, especially since the chasm is on the opposite side of Tethys from the Odysseus Crater. The chasm and surrounding area are heavily cratered, indicating that it was formed a long time ago. (Jaumann et al., 2009). More recent work from the Cassini era (Giese et al., 2007) suggests that Itahca Chasma is older than Oydessus and hence could not have influenced its formation. This work concluded that Ithaca Chasma is an endogenic tectonic feature but the theory is unable to explain why it is confined to such a narrow circular zone.

Tethys has a high geometric albedo, a density close to that of liquid water with many of its crater floors being bright, all of which are suggestive of a composition largely of water ice. Its bright surface is probably also as a result of bombardment of E-ring water ice particles (Verbischer et al., 2007).

Cassini observations revealed that Tethys (like Mimas) has a region of surprisingly high thermal inertia at low latitudes centered on the leading hemisphere (Howett et al., 2012, see Figure 7. This region is correlated spatially with a decrease in the IR/UV surface coloration and the discovery supports the hypothesis that high-energy electrons, which preferentially bombard the leading hemispheres on both Tethys and Mimas, produce clear alterations in texture of the surface. The region is reminiscent of "Pac-Man" just as it is at Mimas. At Tethys, unlike Mimas, the Pac-Man pattern is also observable in visible-light images of the surface, as a dark lens-shaped region and this was first observed by Voyager observations in 1980 (Burns, 1984) but it took higher resolution and the additional instrumentation on Cassini to better understand the implications.

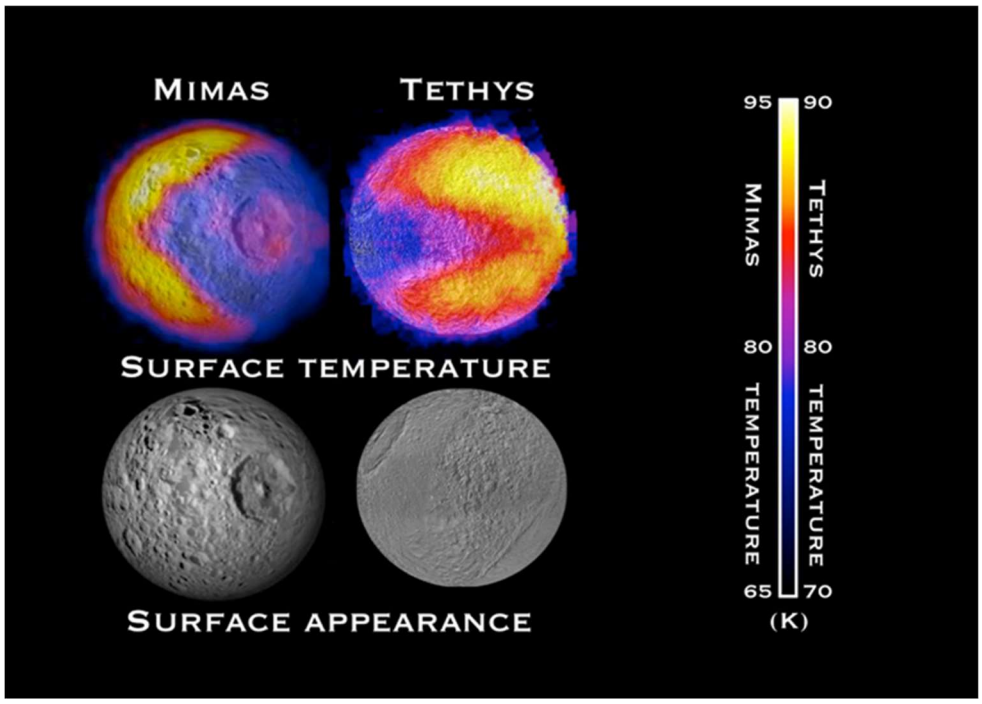


Figure 7: A montage of ISS (visible) images and CIRS (temperature) maps of both Tethys from Sept. 14, 2011, where daytime temperatures inside the mouth of Pac-Man were seen to be cooler than their surroundings by 29 degrees Fahrenheit (15 kelvins). The Mimas Pac-Man shown for comparison is the same data as shown in Figure 6. (PIA 16198, Credit: NASA/JPL-Caltech).

An unusual observation from images taken of Tethys in April 2015, see Figure 8, is that of arc-shaped, reddish streaks which cut across the surface as observed below in the enhanced-color mosaic. These red streaks are narrow, curved lines on the moon's surface, only a few kilometers) wide but several hundred kilometers in length. The origin of these streaks and their color is still a mystery with some ideas including exposed ice with chemical impurities, or outgassing from inside Tethys (Schenk et al., 2005). The yellowish tones on the left side of the view are a result of alteration of the moon's surface by high-energy particles from Saturn's magnetosphere.

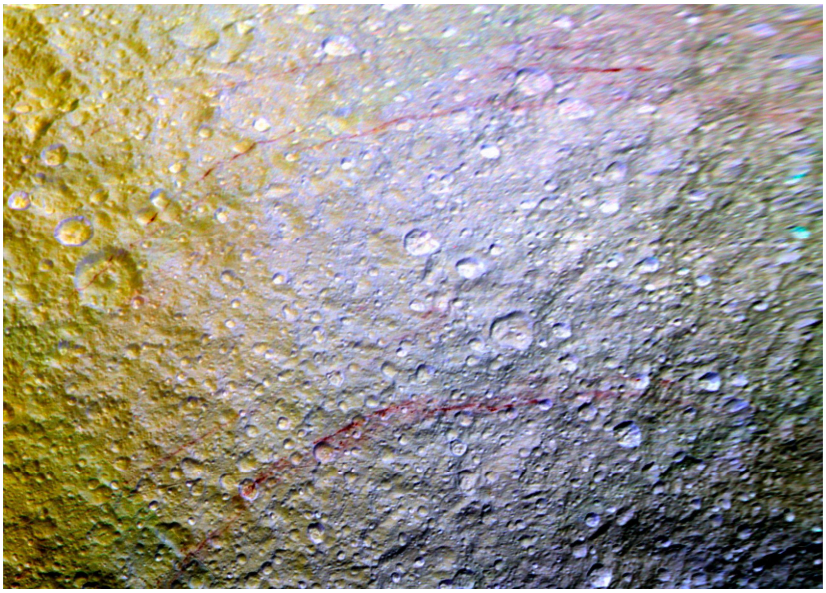


Figure 8: ISS images taken using clear, green, infrared and ultraviolet spectral filters were combined to create this image, which highlights subtle color differences across Tethys' surface at wavelengths not visible to human eyes. The area shown is centered on 30 degrees north latitude, 187 degrees west longitude, and measures 305 by 258 miles across (Credit: NASA/JPL/Space Science Institute).

4.2.3 Dione

There have been 2 targeted flybys of Dione by the Cassini spacecraft and 4 untargeted ones.

Magnetic field observations from the close Dione flyby in October 2005 provided hints of a plasma loading type interaction occurring in the vicinity of the moon (Khurana et al. 2008). The mass loading rates inferred from the observations are rather small (< 7g/s) but the existence cannot be explained from surface sputtering alone. An increase in ion-cyclotron waves close to the position of Dione also indicates that the satellite is acting as a source of a source of newly ionized plasma. This finding was underpinned by observations of molecular oxygen ions on a follow-on close Dione flyby in April 2010 (Tokar et al., 2012) confirming the presence of a very tenuous atmosphere or exosphere.

From improved resolution and global mapping coverage capabilities of Cassini the amount of past endogenic activity on the Dione surface has been one of the surprises. From Voyager it was clear that the surface of Dione was covered by a near global network of tectonic troughs as well as a smooth plain criss-crossed by both ridges and troughs (Jaumann et al., 2009). Cassini confirmed these observations as well as an extension of the smooth plain. In addition the troughs have been revealed to be morphologically fresh (Wagner et al., 2006). Dark material on Dione's surface spectrally matches that seen elsewhere in the Saturn system and Clark et al., 2008a reveal that bombardment by fine particles have impacted the trailing side of the surface, with an external origin for the source being postulated. E ring particles also coat the surface, brightening its albedo.

The origin of wispy streaks on the Dione surface observed by Voyager could not be resolved due to the resolution of the Voyager images (Morrison et al., 1984). The streaks have lengths of tens to hundreds of kilometers and sometimes cut through plains and craters. Cassini observations have revealed that the wispy streaks are in fact bright canyon ice walls (some of them several hundred meters high), probably caused by subsidence cracking. The walls are bright since the darker material falls off them, exposing the brighter water ice beneath (Wagner et al., 2006). The existence of such fracture cliffs suggest that Dione experienced tectonic activity in its past. The density of Dione is almost 1.5 times that of liquid water, suggesting a dense core such as silicate rock and the rest being made up of ice (Morrison et al., 1984).

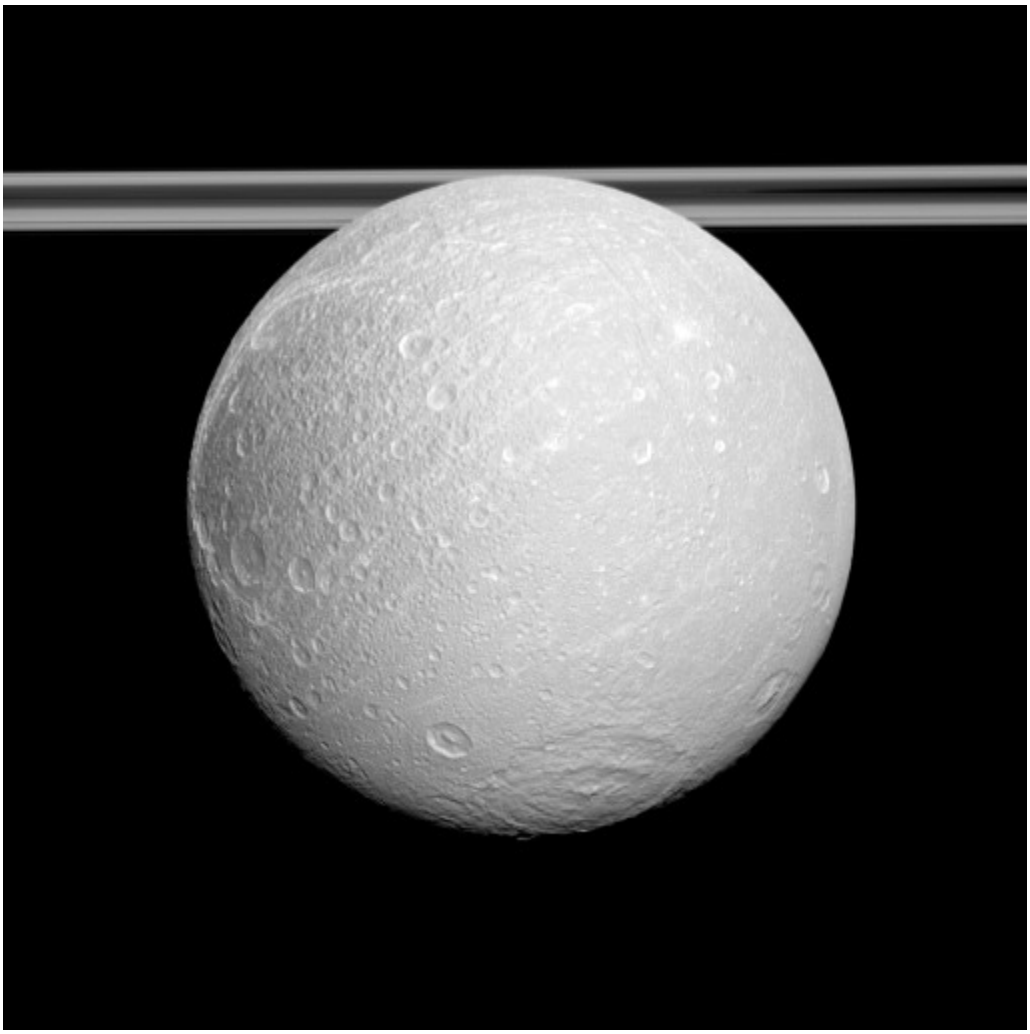


Figure 9: ISS image from the 27th January 2010 non-targeted flyby. This image reveals wispy terrain which winds across the trailing hemisphere of Dione. in this Cassini view taken during the spacecraft's Jan. 27, 2010 non-targeted flyby. This view looks toward the anti-Saturn side (Credit: NASA/JPL-Caltech/Space Science Institute)

Dione is in an orbital resonance with two of the satellites orbiting nearby, that of Mimas and Enceladus. As a result the three moons speed up as they approach each other and slow down as they move apart, a process which assists in keeping them locked into their orbital positions, for example, Dione causes

Enceladus to remain locked at a period which is exactly one half of the Dione orbit (Moore and Wisdom, 2008).

4.2.4 Rhea

The Cassini spacecraft had five flybys past Rhea, two of them targeted and three of them untargeted. As Tethys and Dione are, Rhea is tidally locked in phase with Saturn and it also has a high geometric albedo which suggests a composition mainly of water ice (which at the temperature range of Rhea behaves like rock). Following on from the Voyager era, Rhea was thought to be the least endogenically evolved of the medium sized satellites (Jaumann et al., 2009). Wispy albedo markings were observed in the Voyager images with lengths of tens to hundreds of kilometres sometimes cutting through plains and craters. The Cassini images observed during the 2006 flyby revealed that these wispy areas (as on Dione) are subsidence fractures which form canyons up to several hundred metres high, confirming that Rhea may have been tectonically active in its past (Schenk and Moore 2007; Wagner et al., 2007). The wispy markings are associated with an extensive fault system (similar to Dione) although Rhea does seem less endogenically evolved than the other satellites. Rhea's surface spectra confirm it is mainly dominated by water ice although as with other satellites in the vicinity there is also coating of the surface by E ring particles.

During the 2010 Cassini flyby of Rhea, a very tenuous atmosphere (or exosphere) composed of oxygen and carbon dioxide was detected (Teolis et al., 2010). The exosphere appears to be sustained by chemical decomposition of the surface water ice under irradiation from Saturn's magnetospheric plasma. This discovery of a tenuous atmosphere with oxygen and carbon dioxide makes Rhea unique in the Saturn system.

4.2.5 Iapetus

Our knowledge of Iapetus has greatly improved from the Voyager era following three flybys by the Cassini spacecraft (one targeted and two untargeted). Iapetus has a density only 1.2 times that of liquid water and it is suggested that it (like Rhea) is constituted of three quarters ice and one quarter rock (Castillo-Rogez et al., 2007). Iapetus orbits at 59Rs from Saturn and is therefore less affected by Saturn's tidal forces than the other moons but despite the distance, Iapetus is still tidally locked by Saturn, always presenting the same face to its parent planet. Iapetus is also in resonance with Saturn's largest moon, Titan, which orbits at 20 Rs implying that the two moons speed up and slow down as they pass each other in a complex set of variations. Since Iapetus is less than one third in diameter compared to Titan, the influence on Iapetus is much stronger. Iapetus has been described as the yin and yang of the Saturn moons since its leading hemisphere has a reflectivity (or albedo) as dark as coal whereas its trailing hemisphere is much brighter. The other very unusual feature on Iapetus is the equatorial ridge (Porco et al., 2005) which extends more than half way around its circumference, see Figure 10.

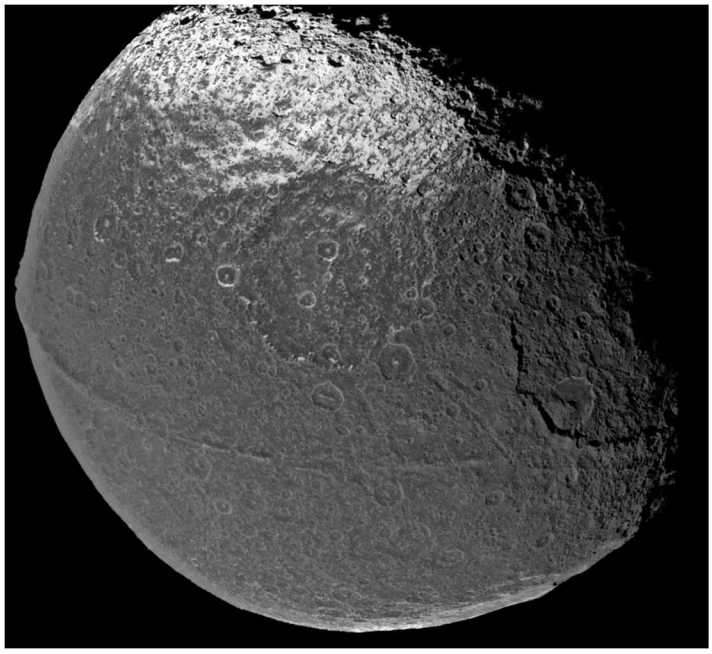


Figure 10: ISS image of Iapetus taken on the 31st December 2004 flyby when the Cassini spacecraft was 172 400km from the moon, the images has a resolution scale of 1km per pixel. (Credit: NASA/JPL/Space Science Institute).

The yin and yang nature of the Iapetus surface (see Figure 11) has been known about since the time of Cassini when he first discovered it and was confirmed by Voyager observations (Morrison et al., 1984) with the possibility been mooted that the satellite may be sweeping up particles from the much more distant (and also dark) moon Phoebe. Such a mechanism would continually renew the dark surface (compatible with the lack of many fresh bright craters within the dark terrain). Another theory is that there may be ice volcanism distributing material such as such as hydrocarbons which will then darken after chemical reactions arise from the effects of solar radiation.

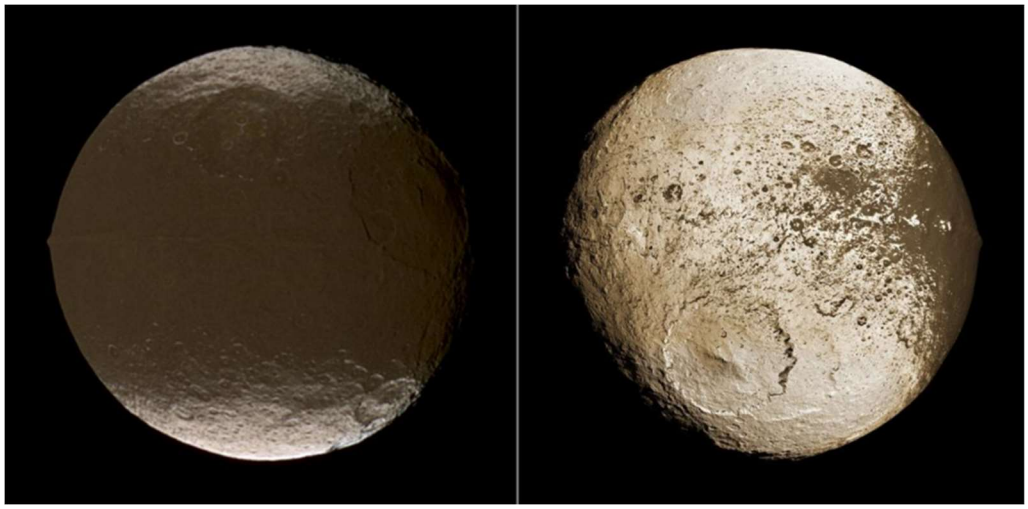


Figure 11: These two global images of Iapetus from ISS show the extreme brightness dichotomy on the surface. The left-hand panel shows the moon's leading hemisphere and the right-hand panel shows the moon's trailing side. (Credit: NASA/JPL/Space Science Institute).

The September 2007 Cassini flyby of Iapetus confirmed that a third process, suggested soon after Cassini arrival at the Saturn system and the first Iapetus flyby in December 2004, thermal segregation, is probably the most responsible for Iapetus' dark hemisphere (Spencer and Denk, 2010). The very slow rotation of Iapetus (79.3 days) is a critical element for this process, since this results in an extremely long daily temperature cycle enabling the dark material to absorb heat an warm up (which it is able to do much better than bright icy material is). Such heating will result in volatile or icy species within the original dark material to sublime out and migrate towards the colder regions on the moon's surface. has a very slow rotation, longer than 79 days. Such a slow rotation means that the daily temperature cycle is very long, so that the dark material can absorb heat from the Sun and warm up. (The dark material absorbs more heat than the bright icy material.) This heating will cause any volatile, or icy, species within the dark material to sublime out, and retreat to colder regions on Iapetus. As a result of this thermal segregation the dark material becomes darker and the bright, cold, neighbouring regions become brighter. For this process of have initiated an influx of a small amount of exogenic dust from some unknown source would have been required to trigger the process.

4.2.6 Hyperion and Phoebe

Our understanding of the two moons Hyperion and Phoebe, with irregular orbits around Saturn has improved during the Cassini era based on observations from five flybys of Hyperion (one targeted and four untargeted) and one targeted Phoebe flyby, the first satellites flyby of the mission which occurred just before Saturn Orbit Insertion.

Hyperion is the largest of Saturn's irregular shaped moons and is thought to be the remnant of a violent collision that shattered a larger moon into different pieces (Matthews, 1992). Its large orbital distance from Saturn and orbital resonance with Titan has stopped it from becoming tidally locked with Saturn and it rotates roughly every 13 days with the orbital period around Saturn of 21 days. We have known about its strange shape, heavily cratered surface and chaotic spin from the Voyager era (Morrison et al., 1984) with Cassini revealing a curious sponge-like appearance (see figure 12) and the presence of complex compounds (Cruikshank et al., 2007). The density of the moon is just over half of that of water

which could be a result of the water ice containing gaps or porosity as well as some lighter materials such a frozen methane or carbon dioxide also being constituents (Thomas et al., 2007). This is compatible with the suggestion that Hyperion accreted from numerous smaller ice and rock bodies without having sufficient gravity to compact the constituents. The sponge like appearance arises since its craters are deep without any clear ejecta rays, although landslides have clearly occurred within some of the larger craters. It has been theorized that the high-porosity and low density of the Hyperion surface would crater as a result of compression from impactors instead of the usual excavation route. An abundance of water ice is implied from the brightness of the majority of the crater walls whereas the floors of the craters are mostly dark perhaps since the temperatures here could cause sublimation of volatiles allowing darker material to accumulate (Jaumann et al., 2009).

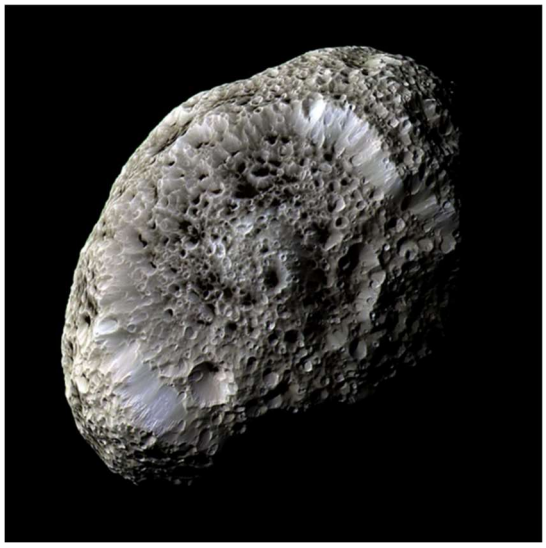


Figure 12: A false-color view of Hyperion obtained during Cassini's close flyby on Sept. 26, 2005. Hyperion has a reddish tint when viewed in natural color, which was toned down to enhance the other hues, showing subtle color variations across the surface. (Credit: NASA/JPL/Space Science Institute).

The surface of Hyperion has a low reflectivity, as does Phoebe and Iapetus (on its dark side). This has been theorized to be for a number of possible reasons including; frozen carbon dioxide mixing with frozen water and other material for example hydrocarbons, or perhaps hydrogen could be being removed by solar radiation from methane in the atmosphere of Titan causing carbon dust to sublimate onto Hyperion, and a third possibility concerns the dark material from Phoebe which has been proposed to color both Hyperion and Iapetus (Jaumann et al., 2009).

Phoebe which is roughly spherical and has a diameter of about 220 kilometers. It has an irregular, elliptical and inclined orbit which is retrograde, the only moon at Saturn which orbits in the opposite direction to the other satellites. Its surface is extremely dark, reflecting only a few percent of the sunlight it receives. The combination of its darkness and retrograde and irregular orbit suggest that Phoebe is probably a captured object from outside of the Saturn system, most likely the outer solar system where dark material is more usual. It could potentially be a captured Kuiper belt object which are believed to be primordial (dating from the formation of the solar system, (Jewitt et al., 2007)). The surface of Phoebe is consistent with a substantial amount of fine grained dust, generated by particle infall (Clark et al., 2008) and also shows signs of a violent collisional history, see Figure 13).

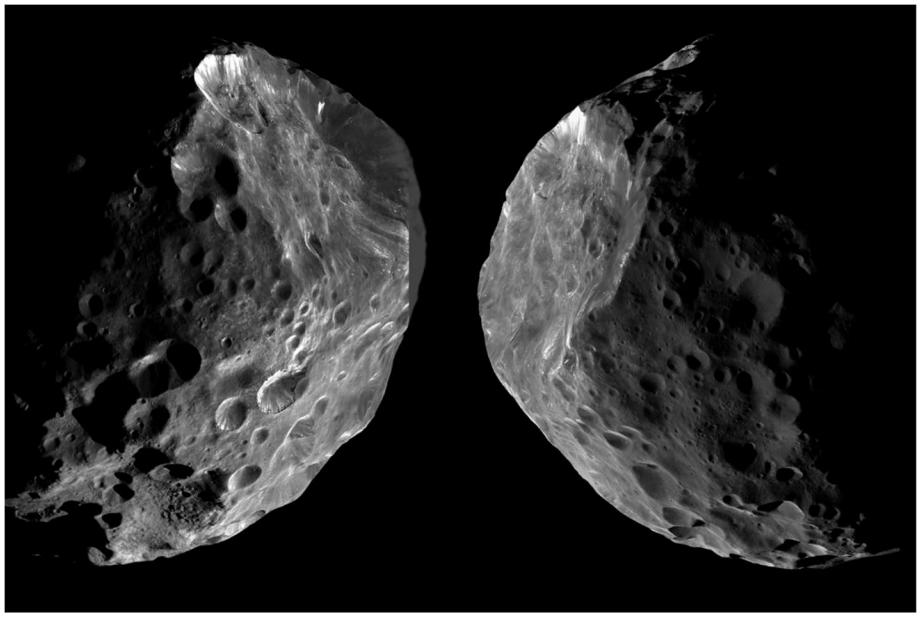


Figure 13: The two ISS images taken on 11th June 2004 as Cassini approached the Saturn system reveal on the left side the view on approach to Phoebe, while the right side shows the spacecraft's departing perspective. (Credit: NASA/JPL/Space Science Institute).

4.2.7 Seven ring region moons: Pan, Daphnis, Atlas, Prometheus, Pandora, and Janus/Epimetheus

The Saturn system contains numerous tiny moons, including seven that orbit close to Saturn's main rings. Some of their key characteristics can be found in (Thomas, 2010).

Pan, the innermost of Saturn's known moons, is a small, ravioli-shaped moon approximately 34 km across. Pan orbits inside the 325-km-wide Encke gap in Saturn's A ring. Pan's gravity creates beautiful wavy edges (wakes) on either side of the Encke gap. The images (see Figure 14, left) show exquisite detail along an equatorial ridge of material circling Pan (Charnoz et al., 2007). Impact craters are visible on both the main body of Pan and on its dramatic, uneven ridge. A landslide from the ridge to the main body is clearly visible in the images.

Daphnis is a tiny potato-shaped moon approximately 8 km across. Daphnis orbits inside the 42-km-wide Keeler gap in the outer portion of Saturn's A ring. The little moon's gravity raises waves in the edges of the gap in both the horizontal and vertical directions (Weiss et al., 2009). A narrow ridge around its equator and a fairly smooth mantle of material on its surface is likely an accumulation of fine ring particles. A few craters are obvious at this resolution. An additional ridge further north runs parallel to the equatorial band.

Atlas is a small saucer-shaped moon about 42 km across and just 18 km pole-to-pole. It orbits just outside Saturn's outer A ring edge. Atlas consists of a central body with an extended ridge of small, icy grains from the rings (Charnoz et al., 2007). The ridge has grown as far as it can grow. Saturn's gravity would pull off any additional ring particles that try to accrete on the edge of the ridge. The ridge is smooth and crater-free. Subtle ridges and grooves wind across its core and may hold clues to Atlas' history and evolution, see Figure 14, right.

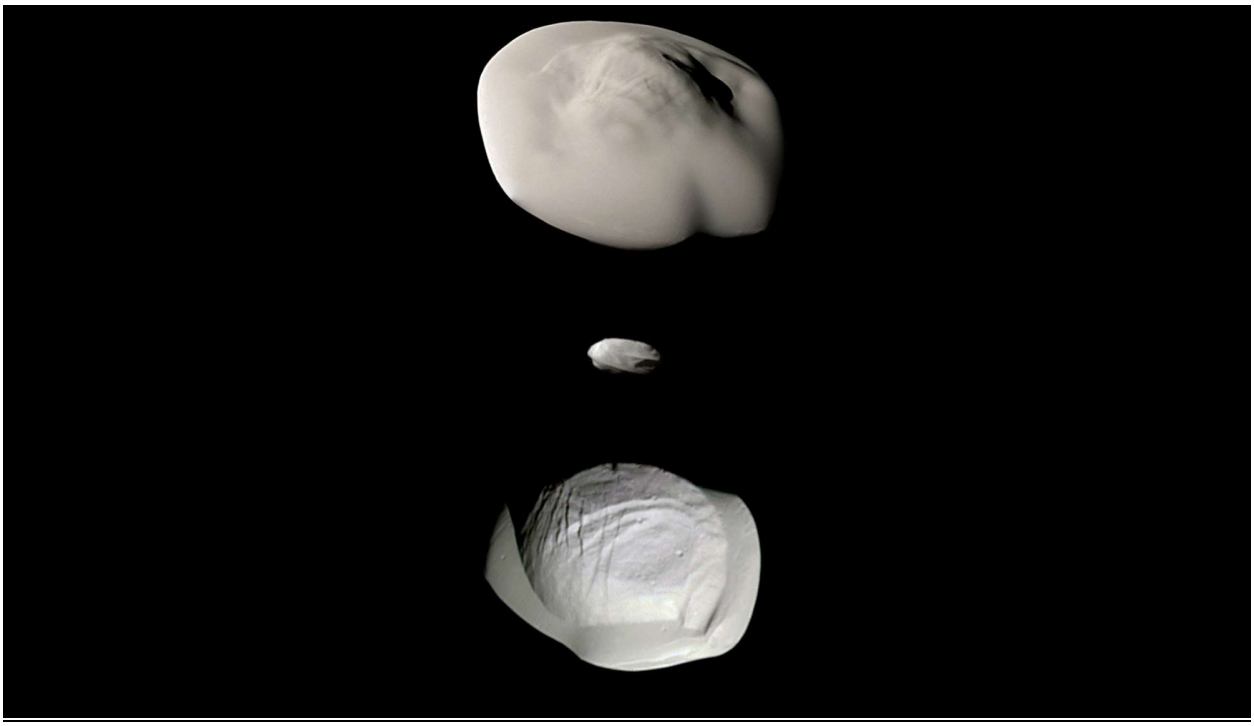


Figure 14: Images of from top, Pan, Daphnis and Atlas show the most detailed views yet of these ring moons as observed by Cassini images from flybys in 2017 (PIA21449 Credit: NASA/JPL/Space Science Institute).

Prometheus is a pockmarked moon about 136 x 79 x 59 km in size. It orbits interior to the F ring and is a shepherd moon for the inner edge of that ring, contributing to the confinement of the F ring (Beurle et al., 2010). Prometheus radically alters the appearance of the F ring, sometimes carving deep channels into the dusty ring material. It has several ridges and valleys as well as a number of impact craters.

Pandora is a potato-shaped, cratered moon about 104x82x63 km in size. It orbits just beyond Saturn's F ring (Beurle et al., 2010). Pandora appears to be covered by fine particles captured from the F ring, and these deposits vary in thickness with location on the satellite. A network of thin, parallel grooves is conspicuous far from Pandora's broad equator, but they appear to vanish under a thick layer of smooth material that blankets the terrain.

Janus-Epimetheus: Janus is a co-orbital moon, sharing its orbit with Epimetheus. Janus has a mean diameter of 180 km while Epimetheus has a mean diameter of 120 km. Janus and Epimetheus orbit too close together to pass one another. Instead, approximately every four years they essentially swap orbits in an intricate cosmic dance as the inner moon overtakes the outer moon, and then switches positions with it, moving to a slower, higher orbit (Lissauer, 1985). The two moons never approach closer than 10,000 km to one another. Cassini observed two such swaps, one in 2006 and another in 2010. Janus and Epimetheus are both heavily cratered, containing several craters larger than 30 km, and both may be quite old. Janus and Epimetheus both have a very low density and are highly porous. They may have formed from the disruption of a single parent body quite early in the history of the Saturn system and may be rubble piles of icy shards.

4.2.8 Small inner system moons: Aegeaon, Methone, Anthe, Pallene, Telesto, Calypso, Polydeuces and Helene

Eight small moons orbit farther from Saturn than the inner ringmoons (Thomas et al., 2010, 2013). Three of these moons, Aegeaon, Methone and Anthe, form a family of moons that orbit between Mimas and Enceladus (Thomas et al., 2013). The other four share orbits with Tethys (Telesto and Calypso) and Dione (Polydeuces and Helene) (Izidoro et al., 2010). Cassini discovered five of these tiny moons (Porco et al., 2005).

Ageaeon is the smallest known moon in orbit around Saturn and was first seen by the Cassini cameras in 2008 (Hedman et al., 2010). It has a very elongated shape, is less than a kilometer in size, and is relatively dark. It orbits within a bright arc of Saturn's G ring and is probably the source of particles for this ring. Aegeaon orbits between Janus/Epimetheus and Mimas.

Methone, Anthe and Pallene all orbit Saturn between Mimas and Enceladus and may once have been part of these much larger moons (Thomas et al., 2013). They orbit close enough together to be part of a dynamical family. Resonances with the much larger moon Mimas strongly perturb the orbits of Methone and Anthe, with the greatest effect on Anthe. Pallene's orbit is perturbed by a resonance with Enceladus. Micrometeoroid bombardment kicks dust off these three moons (Hedman et al., 2007). Partial rings, or ring arcs orbit with Methone and Anthe. Pallene's dust forms a complete diffuse ring, the Pallene ring, about 2,500 km in radial extent around this moon's orbital path. Methone is a smooth, egg-shaped moon with an average diameter of only 3 km, no visible craters and a very low density. Cassini discovered it in 2004 (Porco et al., 2005). Anthe is a tiny moon, only about 2 km in size, discovered by Cassini on May 30, 2007. Once its orbital elements were calculated it was visible in Cassini images all the way back to 2004. Pallene is about 4 km in size and was discovered by Cassini in 2004 (Porco et al., 2005).

Telesto and Calypso both share an orbit with Tethys and are known as Tethys Trojans (Izidoro et al., 2010). Telesto, the leading Trojan, orbits 60 degrees in front of Tethys and Calypso, the trailing Trojan, orbits 60 degrees behind Tethys (Thomas et al., 2010). These stable Lagrange points are created by the gravitational interaction between Saturn and Tethys. Both moons display very smooth surfaces composed of loose material that may help soften and absorb craters (Porco et al., 2007). Telesto is 25 km in size, irregularly shaped, with very few small craters as seen in Cassini images in 2005. Calypso is about 30 km in size and irregularly shaped as seen in Cassini images taken in 2010. Calypso is one of the brightest moons in the solar system, and perhaps because its surface is being blasted by E ring particles from Enceladus. Telesto and Calypso were first discovered in 1980 from ground-based observations (Reitsema, 1981; Veillet 1981).

Polydeuces and Helene both co-orbit with Dione (Izidoro et al, 2010). Helene orbits 60 degrees in front of Dione and Polydeuces orbits 60 degrees behind Dione at the stable Lagrange points described for Telesto and Calypso (Thomas et al., 2010). However, Polydeuces wanders farther from its Lagrange point than any of the other Trojan moons, moving about 30 degrees away from this point in either direction over about two years. Polydeuces is about 3 km in size and was discovered from Cassini images in 2004 (Porco et al., 2007). Cassini was too far away to clearly resolve Polydeuces. Helene is about 35

km in size and was discovered in 1980 in ground-based observations (Lecacheux et al., 1980). It has a smooth, sculpted surface (Porco et al., 2007).

5. What's next for icy satellite science

The rich data set from Cassini will continue to yield high profile science return for many years to come, as well as serve as a training ground for young scientists who will work on the new data sets from up and coming spacecraft missions. The outcome of the Cassini discoveries focused on moon science has raised interest in icy moons (often with subsurface oceans) within our solar system and other planetary bodies, such as exoplanets, beyond our solar system. This interest has prompted studies into follow-up mission concepts, especially future missions to Enceladus and Titan, as well as new selected spacecraft missions to Jupiter's icy satellites.

The first ESA L (large) class mission, JUICE (Jupiter Icy moon Explorer) was selected in 2012, instruments and the spacecraft prime selected and the mission is due for launch in 2022 and will reach the Jupiter system in 2030. This mission will focus on three of the four Galilean satellites at Jupiter, that of Ganymede which it will go into orbit around, Callisto (with 10 flybys) and Europa (2 flybys); as well as spend time within the magnetosphere of Jupiter. The focus of the mission is to understand whether these moons have the potential for habitability .

NASA's Europa Clipper mission will place a spacecraft in orbit around Jupiter to perform a detailed investigation of the moon Europa. It will launch in the early 2020's and upon arrival, perform 45 flybys of Europa at altitudes varying from 25 km to 2700 km above the surface. Europa is a world that harbors a liquid water ocean beneath its icy crust that could contain conditions suitable for life. The mission will send a well-instrumented, radiation-hardened spacecraft into a long, looping orbit around Jupiter, performing repeated close flybys of Europa.

Various mission concepts under study include for Enceladus: a flyby plume sample return, multiple flights through the plume to analyze its content, a surface lander, and astrobiology missions to look for life. Mission concepts for Titan include multiple flybys, an orbiter, lander, balloon, airplane and even a helicopter. Titan's dense atmosphere is an idea place for a balloon, helicopter or airplane to successfully navigate and study Titan's surface. Studies of the other Saturnian satellites have also been a part of other mission concepts as a secondary mission goal.

6 References

Baines, K. H., Flasar, F. M., Krupp, N., and Stallard, T. 2017. Saturn in the 21st Century. Cambridge University Press.

Bouquet *et al.,* 2015*,* Possible evidence for a methane source in Enceladus' ocean ," *Geophysical Research Letters,* March 12, 2015.

Bland, M. T.; Singer, Kelsi N.; et al., 2012. "Enceladus' extreme heat flux as revealed by its relaxed craters". *Geophysical Research Letters*. **39**, (17).

Beurle, K., Murray, C.D., Williams, G.A., Evans, M.W., Cooper, N.J. and Agnor, C.B., 2010. Direct evidence for gravitational instability and moonlet formation in Saturn's rings. *The Astrophysical Journal Letters*, *718*(2), p.L176.

Bond, W.C. 1848. Discovery of a new satellite of Saturn. *Monthly Notices of the Royal Astron. Soc. 9 (1):* 1–2.
Brown, R., Lebreton, J.P. and Waite, J. eds., 2009. *Titan from Cassini-Huygens*. Springer Science & Business Media.
Buratti, B. J. 1988, Enceladus: Implications of it unusual photometric properties, *Icarus, 75*, 113-126.
Burns, J. A. ed. 1977, *Planetary Satellites*, University of Arizona Press.
Cassini, G. D., 1686, An Extract of the Journal Des Scavans. Of April 22 st. N. 1686. Giving an Account of Two New Satellites of Saturn, Discovered Lately by Mr. Cassini at the Royal Observatory at Paris. *Philosophical Transactions of the Royal Society of London*, **16** (179–191): 79–85.
Castillo-Rogez, J. C.; Matson, D. L.; Sotin, C.; Johnson, T. V.; Lunine, J. I.; Thomas, P. C., 2007. Iapetus' geophysics: Rotation rate, shape, and equatorial ridge, *Icarus*, **190** (1): 179–202.
Charnoz, S., Brahic, A., Thomas, P.C. and Porco, C.C., 2007. The equatorial ridges of Pan and Atlas: Terminal accretionary ornaments?. *Science*, *318*(5856), pp.1622-1624.
Clark, R. N., Curchin, J. M., Jaumann, R., Cruikshank, D. P., et al. 2008, Compositional mapping of Saturn's satellite Dione with Cassini VIMS and implications of dark material in the Saturn system, *Icarus, 193,* 372-386
Coates. A.J., Wellbrock, A., Lewis, G.R., Jones, G.H., Young, D.T., Crary, F.J., Waite, J.R., Johnson, R.E., Hille, T.W., Sittler, E.C., 2010. Negative ions at Titan and Enceladus: recent results, Faraday Discuss., 2010, 147, 293–305.
Cruikshank, D. P. et al., 2007, Surface composition of Hyperion, *Nature*, **448**, 54-56.
Cruikshank, D. P. et al., 2008. Hydrocarbons on Saturn's satellites Iapetus and Phoebe, *Icarus*, **193**, 334-343.
Denk, T.; et al., 2010. Iapetus: Unique Surface Properties and a Global Color Dichotomy from Cassini Imaging, *Science*, **327** (5964): 435–439.
Dones, L. et al., Icy satellites of Saturn: Impact cratering and age determination, 2009, Saturn from Cassini-Huygens, Springer Science & Business Media, 613-635.
Dougherty, M. K. et al. 2006, Identification of a dynamic atmosphere at Enceladus with the Cassini Magnetometer. Science 311, 1406–1409.
Dougherty, M., Esposito, L., Krimigis, T. eds., 2009. *Saturn from Cassini-Huygens*. Springer Science & Business Media.
Dyudina, U.A., Ingersoll, A.P., Ewald, S.P., Vasavada, A.R., West, R.A., Del Genio, A.D., Barbara, J.M., Porco, C.C., Achterberg, R.K., Flasar, F.M. and Simon-Miller, A.A., 2008. Dynamics of Saturn's south polar vortex. *Science*, *319*(5871), pp.1801-1801.
Esposito, L.W., Colwell, J.E., Larsen, K., McClintock, W.E., Stewart, A.I.F., Hallett, J.T., Shemansky, D.E., Ajello, J.M., Hansen, C.J., Hendrix, A.R. and West, R.A., 2005. Ultraviolet imaging spectroscopy shows an active Saturnian system. *Science*, *307*(5713), pp.1251-1255
Fletcher, L.N., Irwin, P.G.J., Orton, G.S., Teanby, N.A., Achterberg, R.K., Bjoraker, G.L., Read, P.L., Simon-Miller, A.A., Howett, C., de Kok, R. and Bowles, N., 2008. Temperature and composition of Saturn's polar hot spots and hexagon. *Science*, *319*(5859), pp.79-81.
Fletcher, L.N., Hesman, B.E., Irwin, P.G., Baines, K.H., Momary, T.W., Sanchez-Lavega, A., Flasar, F.M., Read, P.L., Orton, G.S., Simon-Miller, A. and Hueso, R., 2011. Thermal structure and dynamics of Saturn's northern springtime disturbance. *Science*, *332*(6036), pp.1413-1417.
Gehrels, T and Matthews, M. S. , 1984. *Saturn*, University of Arizona Press.
Glein, C. R., Baross, J. A., Waite, J. H., 2015. The pH of Enceladus' ocean. Geochimica et Cosmochimica Acta. 162, 202-219.
Hill et al., 2012, Charged nanograins in the Enceladus plume," Journal of Geophysical Research, 117, A05209, 2012.

Franz, O. G., Millis, R. L. 1975. Photometry of Dione, Tethys, and Enceladus on the UBV system. *Icarus, 24*, 433-442.
Giese, B. et al., 2007, Tethys: Lithospheric thickness and heat flux from flexurally supported topography at Ithaca Chasma, *Geophys. Res. Lett, 34*, L21203.
Goguen, J. 2013. The temperature and width of an active fissure on Enceladus measured with Cassini VIMS during the 14 April 2012 South Pole flyover. Icarus 226, 1128-1137.
Gurnett, D.A., Lecacheux, A., Kurth, W.S., Persoon, A.M., Groene, J.B., Lamy, L., Zarka, P. and Carbary, J.F., 2009. Discovery of a north-south asymmetry in Saturn's radio rotation period. *Geophysical Research Letters*, *36*(16).
Hansen et al.,2011, The composition and structure of the Enceladus plume," Geophysical Research Letters, 38, L11202.
Hansen et al., 2006, Enceladus' water vapor plume," Nature, 311, 5766, 1422-1425.
Hedman, M. M.; Murray, C. D.; Cooper, N. J.; Tiscareno, M. S.; Beurle, K.; Evans, M. W.; Burns, J. A. 2008. Three tenuous rings/arcs for three tiny moons, *Icarus. 199 (2),* 378–386.
Hedman, M.M.; Cooper, N.J.; Murray, C.D.; Beurle, K.; Evans, M.W.; Tiscareno, M.S.; Burns, J.A.. 2010. Aegaeon (Saturn LIII), a G-ring object, *Icarus, 207 (1*), 433–447.
Hedman, et al. 2013, An observed correlation between plume activity and tidal stresses on Enceladus, Nature 500, 182-184 doi:10.1038/nature12371
Helfenstein, P., 2010, Planetary science: Tectonic overturn on Enceladus. *Nature Geoscience* **3**, 75 – 76. doi:10.1038/ngeo763
Hendrix AR, Cassidy TA, Buratti BJ, Paranicas C, Hansen CJ, Teolis B, Roussos E, Bradley ET, Kollmann P, Johnson RE. Mimas' far-UV albedo: Spatial variations. Icarus. 2012 Aug 31;220(2):922-31.
Herschel, W., 1790. Account of the Discovery of a Sixth and Seventh Satellite of the Planet Saturn; With Remarks on the Construction of Its Ring, Its Atmosphere, Its Rotation on an Axis, and Its Spheroidical Figure, Philosophical Transactions of the Royal Society of London, **80,** 1–20.
Howett, C.J.A. , et al. , 2011. High heat flow from Enceladus' south polar region measured using 10–600 cm −1 Cassini/CIRS data. J. Geophys. Res. 116, E03003 .
Howett, C. J. A. et al., 2011. A high-amplitude thermal inertia anomaly of probable magnetospheric origin on Saturn's moon Mimas, *Icarus*, **1**, 221-226.
Howett et al., 2012, PacMan returns: An electron-generated thermal anomaly on Tethys, *Icarus, 221(2),* 1084-1088.
Hsu *et al.,* 2015, Ongoing hydrothermal activities within Enceladus," *Nature,* March 12, 2015.
Iess, L., et al., 2014. The Gravity Field and Interior Structure of Enceladus. *Science*, **344**, 78-80.
Izidoro, A., Winter, O. C., and Tsuchida, M., 2010. Coorbital Satellites of Saturn: Congenital Formation. *Monthly Notices of the Royal Astronomical Society*, **405**(4), 2132–2140.
Jaumann, R. et al., 2009, Icy satellites: geological evolution and surface processes, *Saturn from Cassini-Huygens*. Springer Science & Business Media, 637-681.
Jewitt, D. and Haghighipour, N., 2007. Irregular Satellites of the Planets: Products of Capture in the Early Solar System, *Annual Review of Astronomy and Astrophysics*, **45**: 261–295.
Johnson, Torrence V.; Lunine, Jonathan I., 2005. Saturn's moon Phoebe as a captured body from the outer Solar System, *Nature*, **435** (7038): 69–71.
Kempf et al., 2010. How the Enceladus dust plume feeds Saturn's E ring," Icarus, 206, 2, 446-457.
Khurana, K. K., Russell, C. T. Dougherty, M. K., 2008, Magnetic portraits of Tethys and Rhea, *Icarus, 193*, 465-474.
Kirchoff, M.R. and Schenk, P., 2009. Crater modification and geologic activity in Enceladus' heavily cratered plains: Evidence from the impact crater distribution. *Icarus*, *202*(2), 656-668.
Lassell, W. 1848a. Discovery of a New Satellite of Saturn, *Monthly Notices of the Royal Astron. Soc. 8 (9)*: 195–197.

Lassell, W., 1848b. Names, *Monthly Notices of the Royal Astron. Soc., 8*, 42-3.
Lebreton, J.P., Coustenis, A., Lunine, J., Raulin, F., Owen, T. and Strobel, D., 2009. Results from the Huygens probe on Titan. *The Astronomy and Astrophysics Review*, *17*(2), pp.149-179.
Lecacheux, J., P. Laques, L. Vapillon, A. Auge, R. Despiau, 1980. A new satellite of Saturn, Dione B, *Icarus*, **43**, 111-115.
Lissauer, J.J., Goldreich, P. and Tremaine, S., 1985. Evolution of the Janus-Epimetheus coorbital resonance due to torques from Saturn's ring. *Icarus*, *64*(3), pp.425-434.
Martens, H.R., Ingersoll, A.P., Ewald, S.P., Helfenstein, P. and Giese, B., 2015. Spatial distribution of ice blocks on Enceladus and implications for their origin and emplacement. *Icarus*, *245*, pp.162-176.
Matson, D.L., Spilker, L. J. and Lebreton, J.-P., 2002. The Cassini/Huygens Mission to the Saturnian System. The Cassini-Huygens Mission, Vol. 1, *Space Sci. Rev.,* **104**, Kluwer Academic Publishers, 1-58.
Matthews, R. A. J., 1992. The Darkening of Iapetus and the Origin of Hyperion, *Quarterly Journal of the Royal Astronomical Society*, **33**: 253–258.
McKinnon, W. B., 1985. Geology of icy satellites in *Ices in the Solar System* (Klinger et al. ed), Reidel, 820-856.
Meyer, J. and Wisdom, J. 2008. Tidal evolution of Mimas, Enceladus and Dione, *Icarus*, **193**, 213-223.
Moore, Jeffrey M.; Schenk, Paul M.; Bruesch, Lindsey S.; Asphaug, Erik; McKinnon, William B., 2004. Large impact features on middle-sized icy satellites, *Icarus*, **171** (2): 421–443.
Morrison et al., 1975, Introducing the satellites, in *Planetary Satellites* (J.Burns ed), 3-17.
Morrison et al., 1984, Satellites of Saturn: Geological Perspective, in *Saturn* (Gehrels and Matthews ed.), 609-639.
Morooka, M. W., J.-E. Wahlund, A. I. Eriksson, W. M. Farrell, D. A. Gurnett, W. S. Kurth, A. M. Persoon, M. Shafiq, M. André, and M. K. G. Holmberg, 2011. Dusty plasma in the vicinity of Enceladus, J. Geophys. Res., 116, A12221.
McKinnon, et al., 2015, Effect of Enceladus's rapid synchronous spin on interpretation of Cassini gravity," Geophysical Research Letters, 42, 2137-2143, 2015.
Mitchell, C.J., Porco, C.C., and Weiss, J.W. 2015. Tracking the Geysers of ENceladus into Saturn's E Ring. Astron. Journal, Vol. 149, 156-172.Nimmo, F., Porco, C. and Mitchell, C., 2014. Tidally Modulated Eruptions on Enceladus: Cassini ISS observations and Models. Astron. Journal Vol. 148, 46-60.
Pickering, E. C., 1899. A new satellite of Saturn, *Astronomical Journal*, **20**(458), 13.
Porco, C. C. et al., 2005. Cassini Imaging Science: Initial Results on Saturn's Rings and Small Satellites *Science*, **307**(5713), 1226-1236.Porco, C. C. et al., 2005. Cassini Imagining Science: Initial results on Phoebe and Iapetus, *Science*, **307** (5713): 1237–1242.
Porco, C. C. et al., 2006. Cassini observes the active south pole of Enceladus. Science 311, 1393–1401.
Porco, C.C., P.C. Thomas, J.W. Weiss, D.C. Richardson, 2007. Saturn's Small Inner Satellites: Clues to Their Origins, *Science* **318**, 1602.
Porco, C. et al., 2014. How the Geysers, Tidal Stresses, and Thermal Emission Across the South Polar Terrain of Enceladus are Related," The Astronomical Journal, 148:45-69, doi:10.1088/0004-6256/148/3/45
Postberg, F., et al., 2009. Sodium salts in E-ring ice grains from an ocean below the surface of Enceladus. Nature. 459, 1098-1101.
Postberg, F., Schmidt, J., Hillier, J., Kempf, S., Srama, R., 2011. A salt-water reservoir as the source of a compositionally stratified plume on Enceladus. Nature. 474, 620-622.
Provan, G. et al. 2009, Polarization and phase of planetary-period magnetic field oscillations on high-latitude field lines in Saturn's magnetosphere. *J. Geophys. Res.*, 114.
Reitsema, H.J., 1981. Orbits of the Tethys Lagrangian Bodies, *Icarus*, **48**, 140.

Sayanagi, K.M., Dyudina, U.A., Ewald, S.P., Fischer, G., Ingersoll, A.P., Kurth, W.S., Muro, G.D., Porco, C.C. and West, R.A., 2013. Dynamics of Saturn's great storm of 2010–2011 from Cassini ISS and RPWS. *Icarus*, *223*(1), pp.460-478.
Sayanagi, K.M., K.H. Banies, U.A. Dyundina, L.N. Fletcher, A. Sanchez-Lavega, R.A. West, 2016. Saturn's Polar Atmosphere, Saturn, Cambridge University Press.
Schenk P. M. and Moore, J. M. , 2007. Impact crater topography and morphology on Saturnian mid-sized satellites, 38th LPSC Conference, Houston, abstract 2305.
Schenk P, Hamilton DP, Johnson RE, McKinnon WB, Paranicas C, Schmidt J, Showalter MR. Plasma, plumes and rings: 2011. Saturn system dynamics as recorded in global color patterns on its midsize icy satellites. Icarus. Jan 31;211(1):740-57.
Schenk et al., 2018, Enceladus and the Icy Moons of Saturn (not sure of publishing date yet).

Slipher, E. C, Slipher, V. 1914. Mimas and Enceladus turn always the same face to Saturn. Lowell Observatory Bulletin No. 62. Volume II, 70-72.
Smith, B. A.; Soderblom, L.; et al., 1982. A New Look at the Saturn System: The Voyager 2 Images, *Science*, **215** (4532): 504–37.
Spahn, F. et al. 2006. Cassini dust measurements at Enceladus and implications for the origin of the E ring. Science 311, 1416–1418.
Spencer, J. R. et al., 2006. Cassini encounters Enceladus: background and the discovery of a south polar hot spot. Science 311, 1401–1405.
Spencer, J.R., A.C. Barr, LW. Esposito, P. Helfenstein, A. P. Ingersoll, R. Jaumann, C.P. McKay, F. Nimmo, and J.H. Waite, 2009. Enceladus: An Acitve Cryovolcanic Satellite. Dougherty, M., Esposito, L., Krimigis, T. eds. *Saturn from Cassini-Huygens*. Springer Science & Business Media.
Spencer, J. R. et al., 2010. An unexpected thermal anomaly on Mimas, AAS DPS meeting #42, p942.
Spencer, J. R. and Denk, T., 2010. Formation of Iapetus' Extreme Albedo Dichotomy by exogenically triggered thermal ice migration, *Science*, **327**(5964), 432-435.Spencer, J.R., Nimmo, F., 2013. Enceladus: An Active ice world in the Saturn system. Annu. Rev. Earth Planet. Sci. 41, 693-717. Spilker, L., Ferrari, C. and Morishima, R., 2013. Saturn's ring temperatures at equinox. *Icarus*, *226*(1), pp.316-322.
Spitale, J. N. and Porco, C. C., 2007. Association of the jets of Enceladus with the warmest regions on its south-polar fractures, *Nature, 449*, 695-697.
Spitale*, et al.,* 2015, Curtain Eruptions from Enceladus' South Polar Terrain, Nature, 521, 57–60.
Stone, E. C.; Miner, E. D., 1981. Voyager 1 Encounter with the Saturnian System, *Science*, **212** (4491): 159–163.
Stone, E. C.; Miner, E. D., 1982. Voyager 2 Encounter with the Saturnian System, *Science*, **215** (4532): 499–504.
Teolis, B. D. et al, 2010, Cassini finds an oxygen-carbon dioxide atmosphere at Satunr's icy moon Rhea, *Science, 330*, 1813-1815.
Thomas, P.C. et al., 2007. Hyperion's Sponge-like Appearance, *Nature*, **448** (7149): 50–56.
Thomas, P.C., 2010. Sizes, shapes, and derived properties of the saturnian satellites after the Cassini nominal mission. *Icarus*, **208**(1), 395-401.
Thomas, P.C.; Burns, J.A.; Hedman, M.; Helfenstein, P.; Morrison, S.; Tiscareno, M.S.; Veverka, J. , 2013. The inner small satellites of Saturn: A variety of worlds, *Icarus. 226 (1*), 999–1019.
Thomas, P.C. et al., 2015, Enceladus's measured physical libration requires a global subsurface ocean," 2015. doi:10.1016/j.icarus.2015.08.037
Tiscareno, M.S., and Murray C.D. eds., 2017. *Planetary Ring Systems: Properties, Structure, and Evolution*. Cambridge University Press.
Tobie, G., Čadek, O., & Sotin, C., 2008. Solid tidal friction above a liquid water reservoir as the origin of the south pole hotspot on Enceladus. *Icarus*, *196*(2), 642-652.

Tokar, R. L. et al, 2012. Detection of exospheric O2+ at Saturn's moon Dione, *Geophys. Res. Lett, 39(3).*
Veillet, C. 1981. Locations of Faint objects in the orbits of Tethys and Dione, *Astronomy and Astrophysics*, **102** (1), L5-L7.
Verbiscer, A.; French, R.; Showalter, M.; Helfenstein, P., 2007. Enceladus: Cosmic Graffiti Artist Caught in the Act, *Science*, **315** (5813): 815.
Waite et al., 2006. Cassini Ion and Neutral Mass Spectrometer: Enceladus Plume Composition and Structure. Science 311, 5766, 1419-1422, 2006.
Waite, J. H., et al., 2009. Liquid water on Enceladus from observations of ammonia and 40Ar in the plume. Nature. 460, 487-490.
Waite, J.R., Christopher Glein, C.R., Perryman, R., Ben D. Teolis, B.D., Magee, B.a., Miller, G., Grimes, J., Perry, M.E., Miller, K.E., Bouqet, A., Lunine, J.I., Brockwell, T., and Bolton, S.J. 2017. Cassini Finds Molecular Hydogen in the Enceladus Plume: Evidence for Hydrothermal Processes. Science, Vol. 356, 155-159.
Wagner et al., 2006, Geology, ages and topography of Saturn's satellite Dione as observed by the Cassini ISS camera, *LPSC XXXVII*, 1805.
Wagner et al., 2007, The global geology of Rhea, 38th LPSC conference, abstract 1958.
Weiss, J.W., Porco, C.C. and Tiscareno, M.S., 2009. Ring edge waves and the masses of nearby satellites. *The Astronomical Journal*, *138*(1), p.272.
Yin, A. and Pappalardo, R.T., 2015. Gravitational spreading, bookshelf faulting, and tectonic evolution of the South Polar Terrain of Saturn's moon Enceladus. *Icarus*, *260*, pp.409-439.